SHEAR INSTABILITIES OF WAVE-DRIVEN ALONGSHORE CURRENTS

Nick Dodd[1]
Coastal Group
Hydraulics Research Wallingford
Wallingford, England

Vicente Iranzo
Departament de Física Aplicada
Universitat Politécnica de Catalunya
Barcelona, Spain

Ad Reniers[2]
Faculty of Civil Engineering
Delft University of Technology
Delft, Netherlands

Abstract. The present state of research into and understanding of shear waves is appraised. In this paper these motions, which result from an instability of an alongshore, wave-driven current, are described, their theoretical explanation is recounted, and the history of their discovery is related. The various investigations into their genesis, which attempted to develop an understanding of when and why they occur, are summarized, and more recent research into their finite amplitude development is discussed, focusing on the understanding gained. Attention is also given to observations of shear waves made in the field and attempts to observe them in the laboratory. Finally, work that still needs to be done is described.

1. INTRODUCTION

The nearshore region called the surf zone has been so intensively investigated over the last 30 years, in theoretical and numerical studies, laboratory experiments, and field campaigns, that it is rare nowadays for a completely new phenomenon to be discovered. It was therefore a great surprise to the "nearshore community" to discover that precisely such an event was unfolding when preliminary results of the analysis of data from the SUPERDUCK experiment of 1986 were presented at the American Geophysical Union Fall Meeting in San Francisco, in December 1988. The presentations [*Holman and Bowen*, 1988; *Howd and Oltman-Shay*, 1988; *Oltman-Shay and Howd*, 1988] focused on a remarkable set of measurements made at a depth of 1 m in the trough of a barred beach and in the presence of a substantial longshore current.

The observations were noteworthy for a number of reasons: (1) They were highly coherent, low-frequency, wave-like motions; (2) they occurred apparently only when the longshore current was present; (3) their kinematics were dependent on the longshore current orientation and strength; and (4) these kinematics revealed them to be distinct from any other previously observed nearshore motion.

The observations, which were soon presented in a full journal paper [*Oltman-Shay et al.*, 1989], spanned a period range roughly from 100 to 1000 s and took the form of alongshore propagating, wave-like structures. Such low-frequency motions put them at the low-frequency end of the generally recognized infragravity (IG) band and led to them being characterized as far-infragravity (or FIG) motions (in fact, they were for a while known as FIG waves). They were also remarkable for being highly energetic (rms horizontal velocities exceeding 0.3 m s^{-1} in the presence of a mean longshore current of 0.9 m s^{-1}), as well as being clearly identifiable in time series records of both free surface elevations and, particularly, velocity components (see Figure 1).

However, these motions only occurred in the presence of a strong longshore current, and the stronger the current was, the more energetic the motions were. Furthermore, the motions were remarkable for possessing an alongshore speed of propagation proportional to the longshore current strength and orientation (i.e., they would propagate with the current), and interestingly, all such frequencies would propagate at the same speed, given constant current conditions (i.e., they were nondispersive). Finally, the observed alongshore wavelengths (periods) were between about 50 and 300 m (50 and 1000 s). These properties distinguished the motions from previously recognized IG waves, most notably alongshore propagating edge waves and oblique leaky modes [see, e.g., *Oltman-Shay and Guza*, 1987; *Oltman-Shay and Howd*, 1993]. In fact, these motions possessed a very distinct position in frequency-wavenumber ($\omega - k$) space, as can be seen in Figure 2, and are clearly not (known) leaky or trapped surface gravity modes. (In this

[1]Now at Department of Ocean and Resources Engineering, University of Hawaii at Manoa, Honolulu.

[2]Now at Department of Oceanography, Naval Postgraduate School, Monterey, California.

Reviews of Geophysics, 38, 4 / *November 2000*
pages 437–463
8755-1209/00/1999RG000067*$15.00*
Paper number 1999RG000067

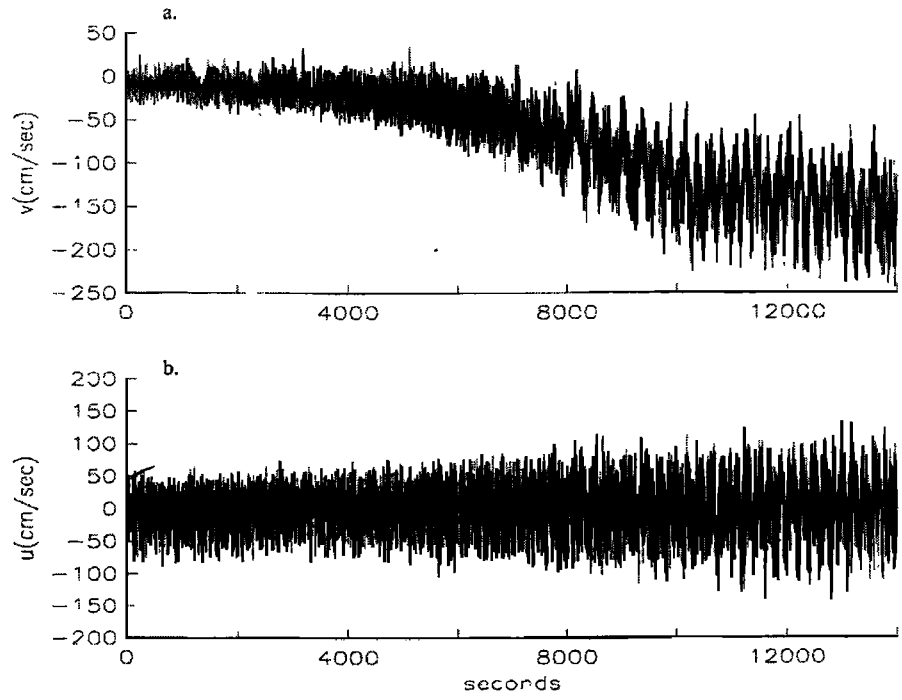

Figure 1. Time series of measurements of (a) alongshore velocity and (b) cross-shore velocity, from a probe located in the surf zone of the beach at the U.S. Army Field Research Facility near Duck, North Carolina, on October 10, 1986, at 0400 LT. From *Oltman-Shay et al.* [1989].

paper we refer to both ω (radial frequency) and $f = \omega/2\pi$ (cyclic frequency, i.e., the reciprocal of the shear wave period). We overwhelmingly use k, the radial wavenumber, although the cyclic wavenumber ($K = k/2\pi$) is referred to in some figures.)

It was therefore apparent that a new phenomenon, or at least one new to the nearshore, wave-dominated regime, had been discovered. The name given to these motions, shear waves, which subsequently came into general usage, reflects the original and convincing hypothesis proposed by *Bowen and Holman* [1989], in a companion paper, that the motions were manifestations of a shear instability of the longshore current.

These types of motions have since been observed during other field campaigns at Duck (DELILAH (1990), DUCK94, and Sandy Duck (1997)), as well as on other days during SUPERDUCK. It is believed that one of the reasons for the auspiciousness of conditions at the Duck site is the presence of a surf zone bar, on which a lot of the incident waves break. This intense breaking generates a strong shear in the longshore current, which is thought to favor instability and the subsequent growth of shear waves (see section 2).

Shear wave like motions have, however, also been observed at other locations, notably on a number of California beaches (see, e.g., *Oltman-Shay and Howd* [1993] and section 4.1), which tend to be more planar as well as steeper. The first (and so far only) laboratory experiments in which these motions have been observed (see *Reniers et al.* [1997] as well as section 4.2) have highlighted this apparent difference between longshore current dynamics on plane and barred beaches, because the shear waves could only be observed when a barred beach was in place.

Interest in these motions is not, however, only an academic one. As was mentioned, these motions are associated with large velocity fluctuations, in both alongshore and cross-shore velocities, and so seem to provide a very potent mechanism for momentum exchanges (or momentum mixing) in the surf zone, which will have a significant impact on the nearshore circulation in general and on the longshore current profile in particular (i.e., the width, shape, and position of the peak in the current). So accurate models of nearshore circulation must consider them. Moreover, such large velocity perturbations can be expected to have a significant impact on cross-shore and longshore sediment fluxes in the surf zone, as well as to alter the mean longshore current profile (which is known to transport large amounts of sediment). They will also affect pollutant and biological dispersion in this zone.

In the next section we develop the fundamental linear theory of these motions, focusing first on idealized models (simplified longshore current and beach profiles) and thereafter examining more realistic conditions, including dissipative mechanisms. In section 3 we review the nonlinear theory, in particular examining the complicated vortex dynamics modeled by fully nonlinear numerical models and examining the capacity for shear waves to mix nearshore momentum. In section 4 we review field experiments at which these motions have been observed, as well as describe the wave basin experiment in which

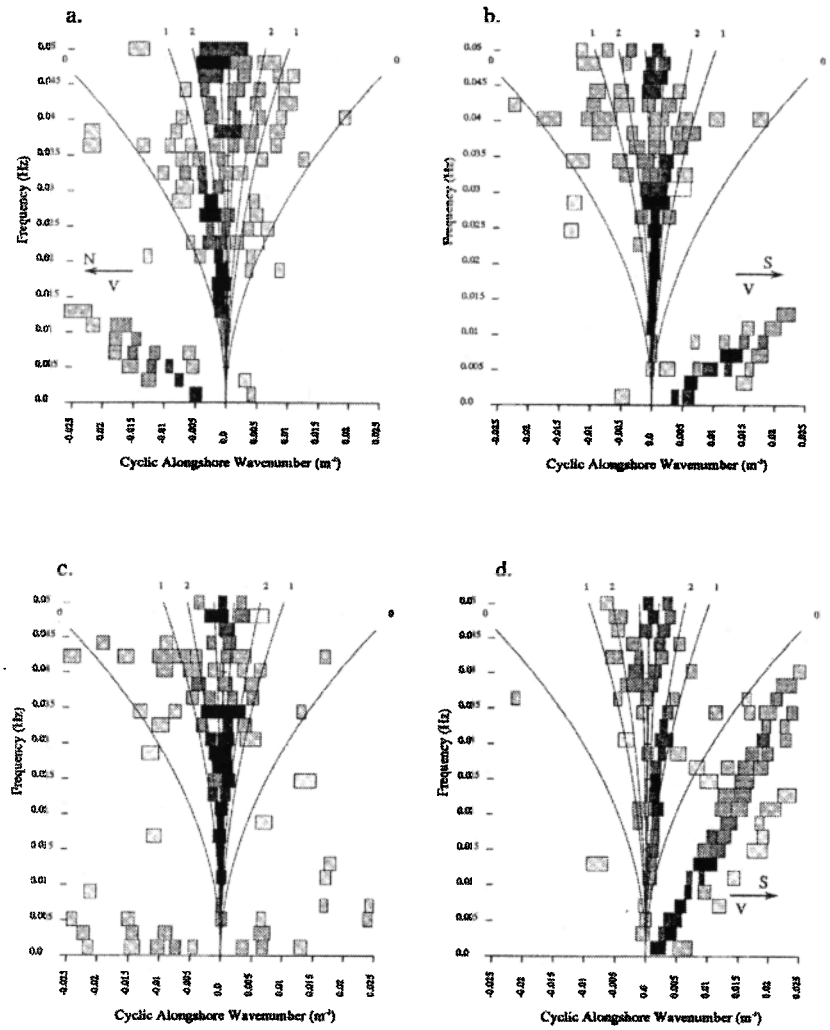

Figure 2. Iterative maximum likelihood estimator estimated f–K spectra of surf zone cross-shore velocity at the U.S. Army Field Research Facility at Duck, on (a) October 9 at 0300 LT, (b) October 11 at 0540 LT, (c) October 11 at 1820 LT, and (d) October 10 at 1030 LT. Rectangles mark the locations of variance peaks, defined as those wavenumber maxima that have an adjacent valley below their half power. Wavenumber width of each box is the half-power bandwidth of the peak. Shading density indicates the percent variance in the frequency bin that lies within the half power bandwidth of the peak. Edge wave dispersion curves (modes 0, 1, and 2) for an effective plane beach slope of 0.055 and leaky-trapped ($\omega^2 = gk$) boundary are plotted. Δf = 0.002 Hz, and degrees of freedom = 56 for all spectra. From *Oltman-Shay et al.* [1989].

these motions have been observed. Finally, we briefly go over other mechanisms that could be responsible for these types of dynamics (section 5) and discuss possible future work (section 6). A brief review of numerical methods and approaches is presented in Appendix A.

2. LINEAR THEORY

A wave-driven, alongshore or longshore current is a fairly common occurrence on many coasts. It is generated by the breaking of surface gravity waves that are traveling obliquely (i.e., wave crests are not parallel to the coastline) to the predominant direction of the coast. The breaking generates cross-shore gradients in the off-diagonal components of the radiation stresses, which therefore dump alongshore directed momentum in the surf zone, creating the current. The situation for a straight, alongshore homogeneous coastline is depicted schematically in Figure 3.

The hypothesis of *Bowen and Holman* [1989] was that this longshore shear flow could become unstable, like any other shear flow, and that the observations of *Oltman-Shay et al.* [1989] were of such an instability. *Bowen and Holman* [1989] presented a simple model, which is nevertheless successful in describing the kinematics and dynamics of these motions. The model considers only the linear shallow water momentum equations

$$u_t + Vu_y = -g\eta_x \tag{1}$$

$$v_t + V_x u + Vv_y = -g\eta_y, \tag{2}$$

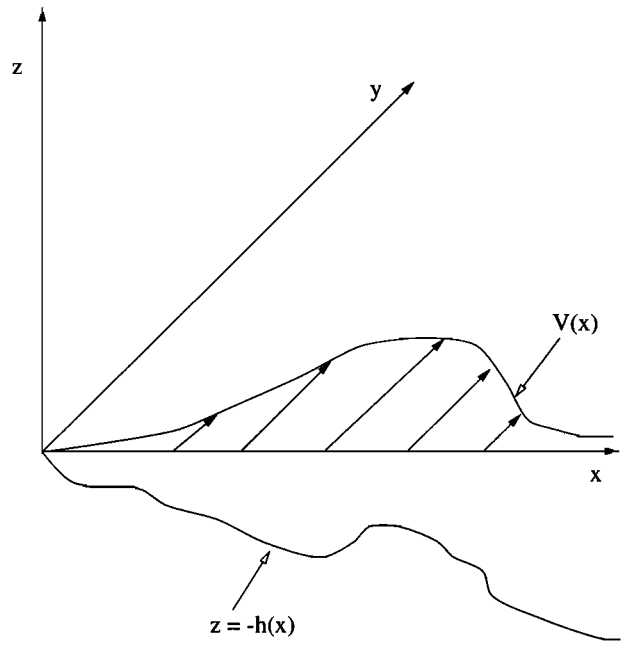

Figure 3. Longshore current profile on an alongshore uniform (barred) beach.

where the total velocity field $(u(x, y, t), v(x, y, t) + V(x))$ consists of a mean, longshore current V and perturbations due to the shear waves (u, v). The $\eta(x, y, t)$ is the free surface elevation associated with these motions. Introducing a rigid-lid assumption (nondivergent flow), a stream function $\psi(x, y, t)$ can be introduced, and we can write

$$u = -\psi_y/h \tag{3}$$

$$v = \psi_x/h, \tag{4}$$

where $h(x)$ is the still water depth. By cross differentiating and eliminating η, an equation for the conservation of potential vorticity is derived:

$$\left(\frac{\partial}{\partial t} + V\frac{\partial}{\partial y}\right)\left[\frac{\psi_{yy}}{h} + \left(\frac{\psi_x}{h}\right)_x\right] = \psi_y\left(\frac{V_x}{h}\right)_x \tag{5}$$

or

$$\frac{D}{Dt}\left(\frac{\Pi + V_x}{h}\right) = 0, \tag{6}$$

where in the linear theory it is understood that only linear terms of (6) are retained. V_x/h represents the background potential vorticity due to the shear in the longshore current, and Π/h is the potential vorticity of the disturbance, so it can be seen that (6) represents a conservation of total potential vorticity. The form (5) is more informative from the point of view of hydrodynamic stability; if the right-hand side of this equation is set to zero, a wave equation results, which describes the advection of neutral disturbances (disturbances neither growing nor decaying) by the current V. So it is therefore the (nonzero) right-hand side of (5) (the coupling between perturbation velocity and the background potential vorticity gradient) that can lead to instability.

The method of normal modes is then used to write ψ as

$$\psi = \phi(x)e^{i(ky-\omega t)} \tag{7}$$

so that (5) becomes

$$(V - c)(\phi'' - (h'/h)\phi' - k^2\phi) = h(V'/h)'\phi, \tag{8}$$

where the prime denotes differentiation with respect to x, which is analogous to the Rayleigh equation [see *Drazin and Reid*, 1981]. Here $c = \omega/k$, and if as is usual, k is assumed real, then the eigenvalue problem (8) (with boundary conditions $\phi(0) = \phi(\infty) = 0$) gives, in general, a complex value for $\omega = \omega_r + i\omega_i$, so that (7) is more informatively written as

$$\psi = \phi(x)e^{i(ky-\omega_r t)}e^{\omega_i t}. \tag{9}$$

Therefore ω_r corresponds to the frequency of the mode (and $c_r = \omega_r/k$ corresponds to a phase velocity), and ω_i corresponds to a growth (or decay) rate (if $\neq 0$). If for a given k, $\omega_i > 0$, then the mode is deemed unstable (it grows without bound); otherwise the mode is said to be stable.

The model of *Bowen and Holman* [1989] uses a very simplified, piecewise longshore current profile (on constant depth) (Figure 4). The complex frequency ω can then be obtained as a function of k by matching solutions in the three regions. The result is a quadratic expression in ω:

$$a\omega^2 + b\omega + c = 0, \tag{10}$$

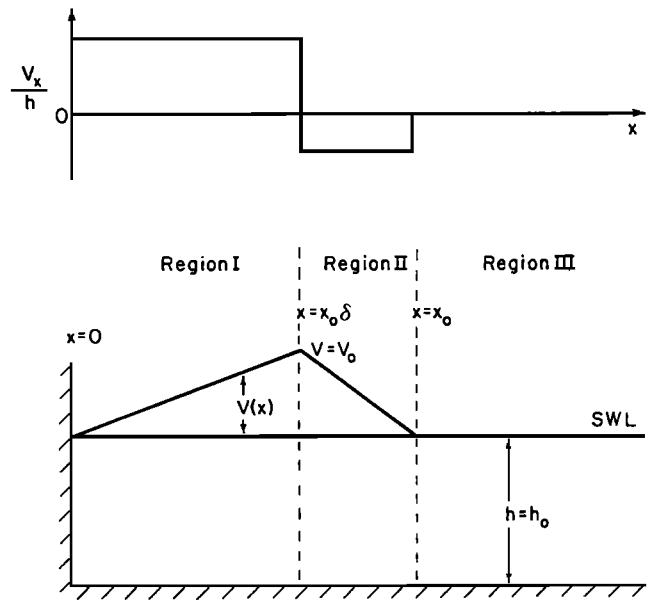

Figure 4. The longshore current profile of *Bowen and Holman* [1989].

where a, b, and c are real. This yields three regions in k space: two in which the roots of (10) are real and a central region in which there are complex conjugate roots. It is therefore only in this latter region that unstable modes can exist, and its size (i.e., the width of the domain of values of k ($k_{\text{lower}} < k < k_{\text{upper}}$) such that ω is complex) depends primarily on the size of the offshore facing or back-shear in the current profile (represented here by δ; see Figure 4) (see Figure 5). Within this range there is a roughly central wavenumber for which the predicted growth rate is a maximum. This unstable mode, $\psi(x, y, t; k = k_{\text{FGM}})$, is often referred to as the fastest growing mode (FGM). (It should, more informatively, be referred to as the fastest growing wavelength (number), since it is merely one point of a continuum of wavenumbers on an instability curve, which itself can be taken to represent one mode. Other modes (separate instability curves) can exist, especially for barred beaches.) Since its growth rate is the largest, according to linear theory it will eventually dominate over other modes. The growth rate of the FGM, and those of all other modes, will also increase with increasing back-shear. *Bowen and Holman* [1989], however, found that the frequency of these motions remains fairly constant, being related primarily to the longshore current strength.

The FGM possesses a wavelength of about 250 m and a period of about 750 s [*Bowen and Holman*, 1989]. For this wavelength the stream function is reconstructed (from equation (7)) and is shown in Figure 6, along with the total velocity field. The meandering of the current due to the shear waves is apparent, and the whole pattern propagates in the direction of the longshore current.

For the parameter values shown in Figure 4, unstable wavenumbers exist in a region $190 < \lambda < 435$ m (where $\lambda = 2\pi/k$). The corresponding range of periods is about 550–1000 s. Therefore the waves propagate with a velocity between one quarter to one half the peak longshore current velocity V_{max}.

Bowen and Holman [1989] estimate rough scales for the growth rate of the FGM of between 0.1 and 0.2 times the maximum back-shear, with frequencies about 0.07 times this back-shear value. Similar inviscid calculations, but for more realistic $V(x)$ profiles, show similar results (*Falqués and Iranzo* [1994] find FGM growth rates of between 0.06 and 0.15 times the back-shear, with frequencies of 0.08–0.1 times). While the predicted inviscid frequencies are largely insensitive to dissipative effects, the growth rates are strongly affected by the introduction of dissipation.

2.1. Realistic Conditions and the Effects of Dissipation

The main limitations of this linear model (similar models have been presented by *Dodd and Thornton* [1990] and *Deguchi et al.* [1992]) are that it does not consider dissipative effects and that the highly simplified

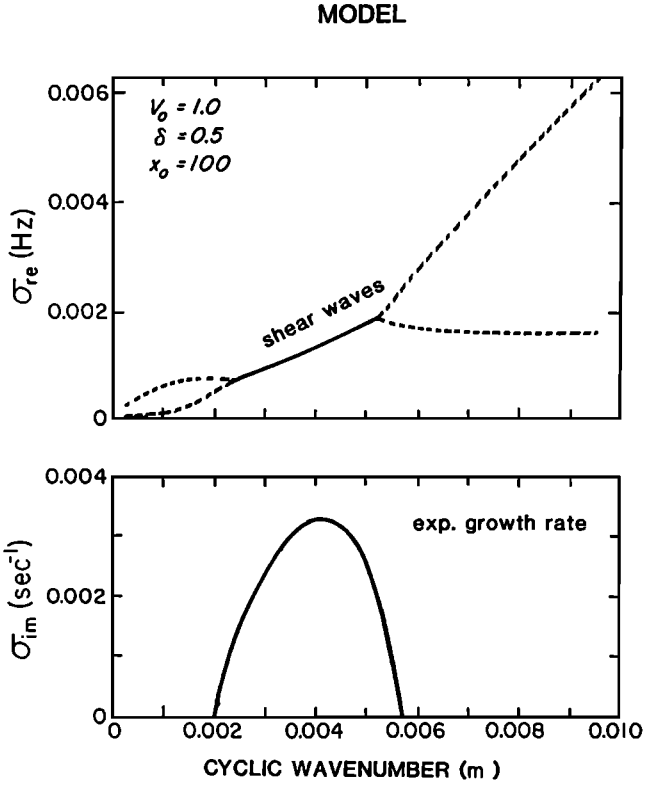

Figure 5. Frequency-wavenumber plots of the shear instability for the geometry shown in Figure 4. Top panel shows components, and lower panel shows imaginary components. Wave motions for which $\omega_i > 0$ ($\sigma_{im} > 0$ in the figure) are unstable. From *Bowen and Holman* [1989].

form for the longshore current gives a limited span of unstable wavenumbers. Observations tend to show instabilities at lower frequencies (wavenumbers), and more realistic beach and longshore current profiles ($h(x)$ and $V(x)$) give a larger range of unstable wavenumbers, stretching, in the absence of dissipative mechanisms, over a region $0 < k < k_{\text{upper}}$ (see Figure 7). Dissipation tends to reduce growth rates fairly uniformly over the range of unstable wavenumbers, in effect pulling the growth rate curve down so that once again a region $k_{\text{lower}} < k < k_{\text{upper}}$ appears (see Figure 7).

Dodd and Thornton [1990] also examine a piecewise longshore current and beach profile, though one slightly more realistic than that of *Bowen and Holman* [1989]. They obtain results similar to those of the earlier authors, indicating (as noted by *Falqués and Iranzo* [1994]) that a nonzero depth at the shoreline is not crucial in obtaining realistic $\omega - k$ curves (i.e., one with $(0, 0)\omega - k$ intercepts), but that it is rather the piecewise nature of the profiles that lends them this slightly unrealistic quality (compared with more realistic profiles).

Within the surf zone, dissipative mechanisms are clearly important, even though shear wave motions occur at timescales and length scales very different from surface gravity waves. The two main dissipative mechanisms are bed shear stress, which in the steady state has

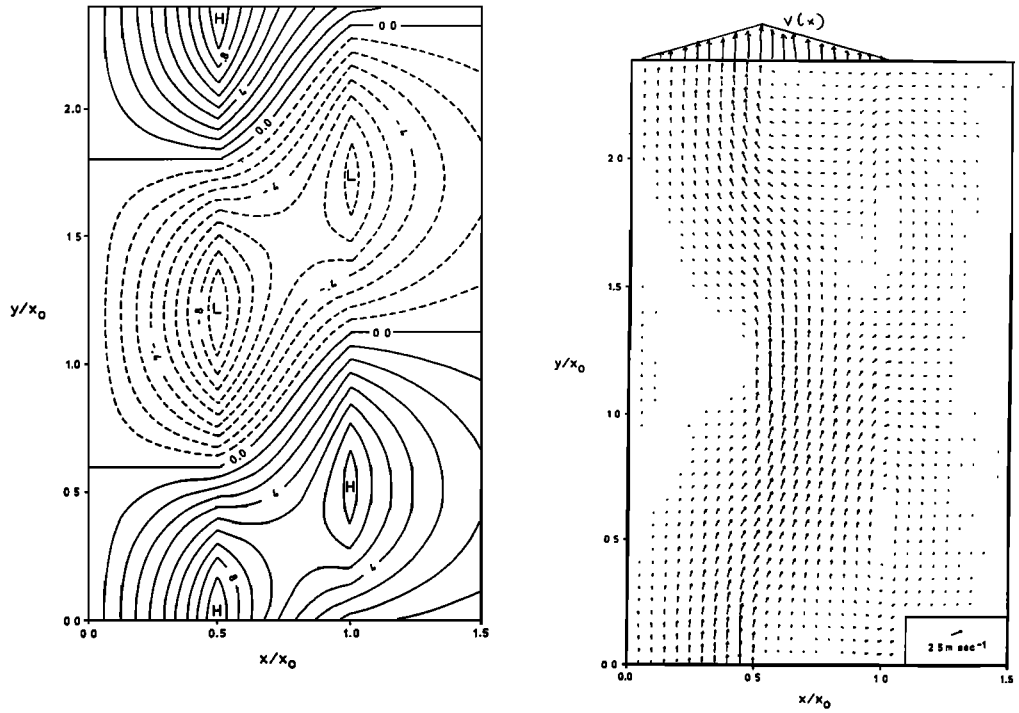

Figure 6. (left) Stream function pattern for one wavelength of a shear wave. (right) Total velocity pattern for one wavelength of a shear wave. The shear wave has been scaled so that its peak magnitude equals the peak alongshore current V_0. From *Bowen and Holman* [1989].

the effect of balancing the mean current itself, and some form of momentum diffusion (eddy viscosity), which acts to smooth out the flow in the cross-shore direction. Their absence from the *Bowen and Holman* [1989] model leads to a prediction of instability of the current for any conditions, which does not tally with observations.

The inclusion of bed shear stress and lateral diffusion terms in (1) and (2) gives us

$$u_t + Vu_y = -g\eta_x - \tau_{b1} + \tau_{d1} \tag{11}$$

$$v_t + V_x u + Vv_y = -g\eta_y - \tau_{b2} + \tau_{d2}, \tag{12}$$

where τ_{bi} are the linearized components of the bed shear stress, which are typically parameterized through a friction coefficient, c_d; and τ_{di} are similar components of the momentum diffusion term, represented through an eddy viscosity coefficient ν.

Dodd et al. [1992] introduced bottom friction into the modeling and analyzed realistic longshore current profiles obtained from two different sites. Their comparison of theory and observation strongly reinforces the hypothesis of *Bowen and Holman* [1989]. *Dodd et al.* [1992; see also *Dodd et al.*, 1990] perform a detailed comparison between observations made during SUPERDUCK and predictions provided by linear stability theory. They use measured beach profiles for 4 days of that experiment, along with the measured $V(x)$ profiles. (Because these profiles consisted of only between three and six points, the profiles were constructed by using the model of *Whitford and Thornton* [1996], which was calibrated using the measured data, and one profile was generated for each measurement, since measurements were sequential.) Overall they found good correlation between

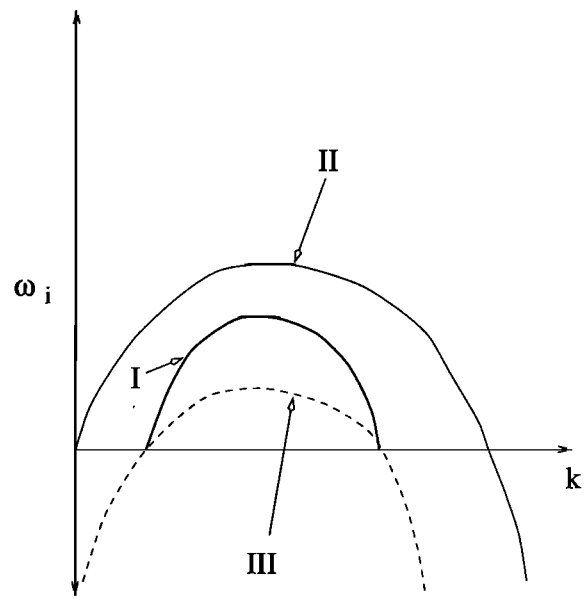

Figure 7. Depiction of growth rate curves. Curve I indicates simplified, piecewise V and h profiles, without dissipation. Curve II indicates realistic, smooth V and h profiles, without dissipation. Curve III indicates realistic, smooth V and h profiles, with dissipation.

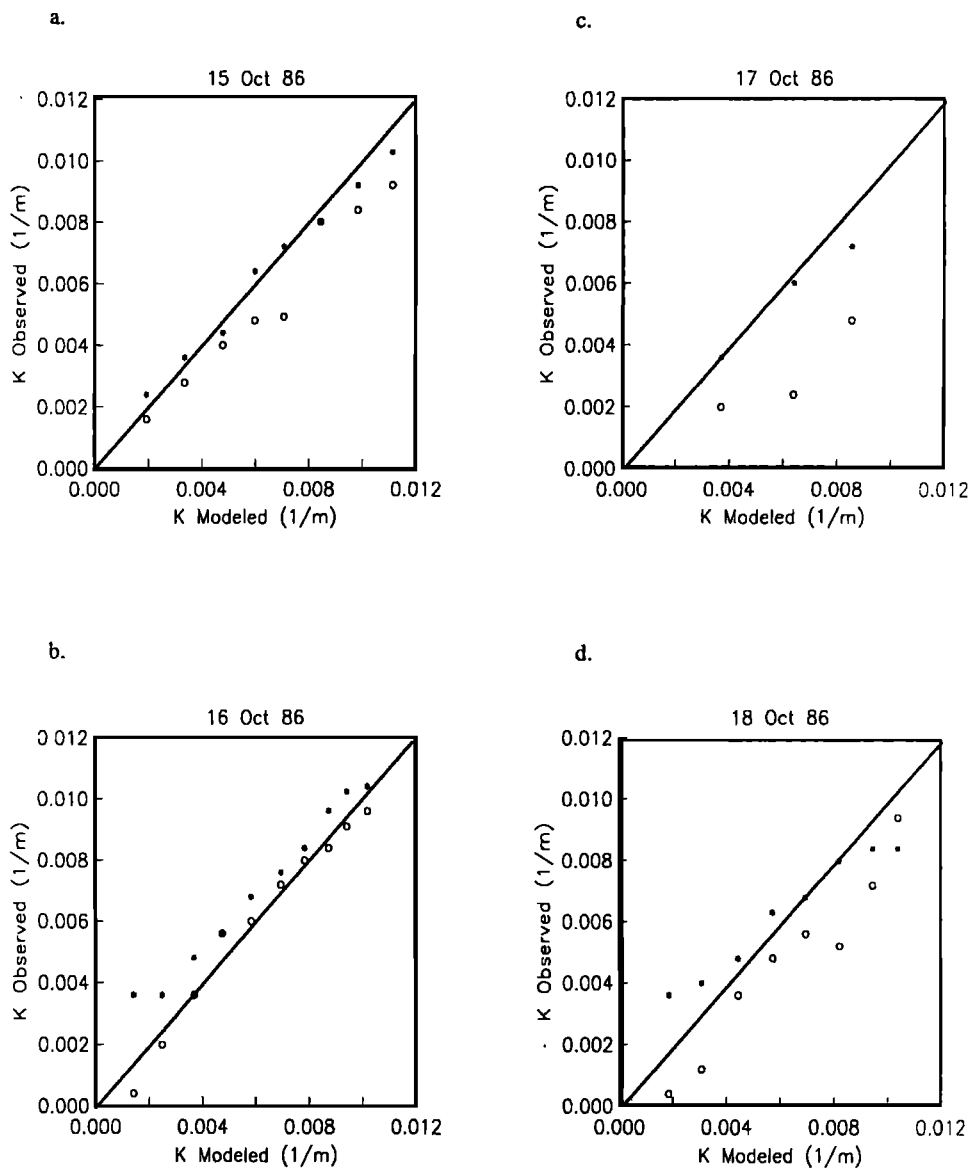

Figure 8. Correlation between predicted (modeled) and observed cyclic wavenumber (m^{-1}) for (a) 15 October, (b) 16 October, (c) 17 October, and (d) 18 October at SUPERDUCK. Observed peak cyclic wavenumbers from cross-shore velocity $f - K$ spectra are shown by asterisks, and those from alongshore velocity $f - K$ spectra are shown by circles. Reprinted from *Dodd et al.* [1992] with permission from the American Meteorological Society.

the observed and computed unstable wavenumbers (see Figure 8) and good agreement between observations and theory on the overall range of unstable wavenumbers (over which range shear wave motions are observed) and on the phase speed of the shear waves. They also compare the observed variance densities of the alongshore and cross-shore velocity components with the calculated growth rates as a function of the predicted frequency for each day. Although there is no quantitative comparison to be made thereby, because the growth rates are dimensionally different from the variances, the overall functional dependence and frequency range of the growth rates is reasonably close to the observed variances, particularly for the cross-shore velocity components, which indicates that even though observations are most likely of finite amplitude shear waves, the most energetic wavelengths correspond roughly to those of the FGM. They note that the predicted growth rates are likely to provide a spinup time during which the shear waves achieve some sort of finite amplitude, and they find that for most days this time was between 300 and 400 s, which translates into a distance of about 250–350 m: 1–2.5 wavelengths. In other words, the growth rate is substantial and the assumption of linearity is limited, a fact previously noted by *Bowen and Holman* [1989] (see also section 3).

In their analysis of the measured profiles, *Dodd et al.* [1992] note the presence of two distinct unstable modes

(instability dispersion curves). They find that the largest growth rates are associated with the unstable mode that has a maximum close to the bar crest, which is associated with the extremum in potential vorticity there. In fact, linear instabilities may be associated with any local extremum in the background potential vorticity, whether on the back-shear or the front (shore facing) one [*Dodd et al.*, 1992; *Putrevu and Svendsen*, 1992] (see also section 2.2).

Putrevu and Svendsen [1992] subsequently undertook a parametric investigation into the effect of different beach profiles (horizontal, plane, equilibrium, and barred) and the position of the longshore current maximum on the linear stability of the current. They confirm the speculation of *Bowen and Holman* [1989] and the findings of *Dodd et al.* [1992] that the bar significantly destabilizes the current. They also note that on a barred beach more than one unstable mode may exist. In particular, they show that one of these modes is similar in $\omega - k$ space and in eigenfunction structure to that on a plane beach. This mode is most energetic seaward of the breakpoint. Typically, however, a second unstable mode can also be excited. This mode will have a different signature in $\omega - k$ space (although the dispersion relation will still be linear), and importantly, will be most energetic at or shoreward of the breakpoint; in effect, it will be trapped by the bar [see also *Dodd et al.*, 1992]. It is this mode that is associated with growth rates larger than those for the plane beach (for identical $V(x)$) for smaller wavelengths and which is believed to be particularly prone to excitation over the barred beach and may in part explain why barred beaches may show more evidence of shear waves than plane ones. The other reason is the larger offshore shear associated with the mean longshore current. They also find that the position of the bar crest relative to the current is the main arbiter of whether or not the "bar-trapped" mode is excited or not. The actual beach slope has very little effect on the stability of the current. (It is important, however, to keep in mind that the study of *Putrevu and Svendsen* [1992] is a parametric one. In other words, they imposed current profiles on a bathymetry, which would not necessarily be those resulting from a given bottom profile and any realistic wave condition.) *Putrevu and Svendsen* [1992] find that the phase speed of the shear waves is about $0.5V_{\max}$.

The effect of bottom shear stress on the shear waves was examined in more detail by *Dodd* [1994]. The effect of this dissipation is twofold: to reduce the longshore current strength, and therefore the shear, and to directly damp instabilities. *Dodd* [1994] investigated this by considering consistent values of the bottom friction coefficient both for the longshore current profile and for the instabilities. The effect of friction on the stability curves is to reduce the span of unstable wavenumbers and the growth rates. There are other bottom friction effects, however, linked to the curvature of the flow, which act to destabilize the current. It was also shown that a global cutoff frequency could exist, below which no linear instability can develop. This is because as the bottom friction coefficient c_d is decreased, thus increasing the tendency to instability, the lower limit of the unstable band of wavenumbers $k_{\text{lower}} \rightarrow 0$, thus allowing lower frequencies to become linearly unstable. However, as $c_d \rightarrow 0$, the longshore current $V(x)$ increases uniformly, and since the frequency of the instabilities $\propto V(x)$, there may be a frequency below which no instability can exist, depending on the relative rates. It was found that such periods exist (at 580 and 458 s for the two profiles examined by *Dodd* [1994]). Such a cutoff, however, has not been observed in the field, although resolution at such low frequencies is usually poor. *Shrira et al.* [1997] have since provided a theoretical explanation of this, based on the emergence of different types of instabilities; see section 3. Examining two different $V(x)$ profiles, *Dodd* [1994] also shows that destabilization occurs for very similar values of the current back-shear.

How the term τ_b is linearized affects the form of the resulting stability equation, but *Dodd* [1994] found that the differences, most obviously due to linearizations based on a weak or strong longshore current [*Liu and Dalrymple*, 1978], are not crucial. In fact, its effect can most simply be incorporated into (8) as

$$(V - c - i\mu/kh)(\phi'' - (h'/h)\phi' - k^2\phi) = h(V'/h)'\phi, \tag{13}$$

in which its effects on growth rates $c_i k$ are plainly appreciated. The effect of a nonconstant friction coefficient $\mu = \mu(c_d; x)$ has also been examined [see *Dodd and Falqués*, 1996] and has been found to be qualitatively similar to the constant coefficient case.

The validity of the rigid-lid assumption implicit in (3) and (4) has been examined in detail [*Falqués and Iranzo*, 1994]. This assumption is based on a local Froude number, $F = V_0/\sqrt{gh_0} \ll 1$, where V_0 and h_0 are representative local values. Physically, this condition states that shear wave motions, whose phase velocity scales with the current strength, may be decoupled (to a first approximation) from shallow-water surface gravity motions, as they possess much slower intrinsic velocities. For a Froude number $F < 0.6$, which condition pertains for most natural beaches, growth rates need only be corrected by less than 12% (shown by *Falqués and Iranzo* [1994] by comparing solutions with and without the imposed rigid lid). This correction, interestingly, is in the form of a stabilization (decrease in growth rates), which, in line with previous authors [see *Dodd and Thornton*, 1990; *Putrevu and Svendsen*, 1992], they ascribe to the increasing interaction of shear wave and gravity wave modes as F increases, resulting in energy being fed into gravity modes.

The study of *Falqués and Iranzo* [1994] was the first to consider the effect of lateral momentum diffusion (eddy viscosity) on the shear instabilities. They find that it, too, damps the shear waves. They also noticed, however, that

the damping induced by an eddy viscosity is highly dependent on the cross-shore position x_{max} of the longshore current maximum V_{max}. *Falqués et al.* [1994] investigate this further, introducing a nonconstant eddy viscosity coefficient $\nu(x)$ and note that initially an increase in eddy viscosity could increase growth rates. This happens if the eddy viscosity profile has its maximum around x_{max} and a rapid decay offshore. One explanation of this can be seen by noting that the gradient in the diffusion coefficient results in wave-propagating terms $(\nu_x \partial_{x_i})$, which act to propagate disturbances. In such circumstances they conclude that the damping effect is actually initially outweighed by an effect of the nonconstant viscosity coefficient (resulting in a destabilization), although further increases in ν always ultimately damp instabilities. *Caballería et al.* [1997] subsequently presented a simplified model to illustrate this effect and came to the same conclusions, and *Putrevu et al.* [1998] look at a similar problem and come largely to the same conclusion. *Putrevu et al.* [1998] examine the less realistic *Bowen and Holman* [1989] profile but more interestingly, note that the argument of *Lin* [1967] may explain the apparent destabilization even without an eddy viscosity gradient. (*Lin* [1967] notes that phase changes in velocity components induced by the introduction of viscosity act to extract energy from the mean flow (here the longshore current). *Putrevu et al.* [1998] show that the introduction of eddy viscosity within their simplified system increases the size of the energy production/extraction term in the energy equation for the perturbed motions.) More recent work on more realistic current profiles [*Dodd and Iranzo*, 1999] appears tentatively to concur.

Note also that with the inclusion of eddy viscosity, the Rayleigh-type equation (13) is transformed into one of Orr-Sommerfeld type. Other, nonlinear studies have revealed a purely or at least an overwhelming damping effect of eddy viscosity, whether they used a constant eddy viscosity coefficient [*Deigaard et al.*, 1994] or a cross-shore varying one [*Özkan-Haller and Kirby*, 1999]. The conclusion seems to be that at least for realistic conditions, eddy viscosity provides only damping, as would be expected.

Predictions of phase speeds, c_r, by linear models largely fall into a range $0.25 < c_r/V_{max} < 0.8$, with more realistic profiles tending to give estimates toward the higher end of this range. The observations of *Oltman-Shay et al.* [1989] of phase velocity were made with respect to a mean current at one location (i.e., bar trough). Although it is not clear whether V_{max} is situated in the trough for all the days they examined, it is known that the longshore current maximum was located over the bar for most of the days of SUPERDUCK. A simple estimate of observed phase speeds relative to V_{max} then gives $c_r/V_{max} \approx 0.55$, which is consistent with those estimates from linear theory [see *Falqués and Iranzo*, 1994]. (The range of values of c_r/V_{max} given by *Falqués and Iranzo* [1994] for the study of *Dodd et al.* [1992] (0.6–0.9) is perhaps a little high. By studying Figure 6 of *Dodd et al.* [1992] (October 16, 1986), a value of $c_r/V_{max} \approx 0.7$ can be calculated. Estimates from Dodd et al.'s Figures 7–10 are more difficult to make because of the representation of the data in those figures.) Dissipation was found to have little effect on the phase speed or frequencies; *Falqués and Iranzo* [1994] find a decrease of less than 9% in frequencies due to the presence of dissipation. The nonlinear study of *Özkan-Haller and Kirby* [1999] also found that eddy viscosity does not seem to affect phase velocities; see section 3.2.

Falqués et al. [1994] also developed stability parameters based on both bottom friction and eddy viscosity. The idea was to provide crude predictions, based on estimated values for c_d and ν, that would indicate whether or not a particular longshore current was likely to exhibit instability, even if direct measurements of shear waves were not available (see section 4).

2.2. Necessary Conditions for Instability

As in the classical stability theory [see *Drazin and Reid*, 1981], there are a number of theorems that can be proved, which demonstrate necessary conditions for a flow to be unstable.

Bowen and Holman [1989] note that a necessary condition for instabilities to grow is that there must be a local extremum in potential vorticity, V_x/h. *Dodd and Thornton* [1990] also show that a necessary condition for instabilities to develop is that $0 < c_r < V_{max}$, again in line with results from classical stability theory. They also demonstrate analytically that motions can be expected to be nondispersive to leading order. *Putrevu and Svendsen* [1992] prove the equivalent result to Fjørtoft's theorem: $(V_x/h)_x(V - V_s) < 0$ in some part of the domain for an instability to exist, where V_s is the longshore current value at a location where an extremum in potential vorticity exists ($(V_x/h)_x = 0$). *Falqués and Iranzo* [1994] prove the analogous result to Howard's semicircle theorem [see *Howard*, 1961; *Drazin and Reid*, 1981] but with the inclusion of both nonconstant depth and a free surface (no rigid-lid assumption). They also derive an analytical estimate for phase speed of neutral shear waves: The phase speed of the neutral wave $c_{ne} = V(x_s) = V_s$, where x_s is the cross-shore position of the aforementioned extremum in potential vorticity. This estimate only applies to neutral (neither growing nor decaying) waves, but it is reasonably robust: For a plane beach this estimate exceeds the computed one by 13%, and for a barred beach the estimate exceeds the computed one by 30%.

It is also straightforward to show that a necessary condition for the instabilities to develop (as opposed to decay) is that the cross-shore gradient of the horizontal Reynolds stresses be nonzero, specifically that the Reynold's stresses must be negatively correlated with the longshore current shear [*Dodd and Thornton*, 1990]. This has important consequences for mixing of momentum in the nearshore region (see section 3).

2.3. Spatial Instabilities

Until now, the only linear theory considered has been the temporal instability theory, in which k is assumed real and ω is complex. However, it is also possible to take ω as being real and find the complex $k = k_r + ik_i$ from the eigenvalue problem, i.e.,

$$\psi(x, y, t) = \phi(x)e^{i(k_r y - \omega t)}e^{-k_i y}. \quad (14)$$

These modes are referred to as spatial modes, because they grow in space (for a fixed time). These modes are also sometimes thought to be more physically realistic than temporal modes (for instance, if instabilities grow from a specific point in space [see *Reniers et al.*, 1997]); however, the mathematical theory is more complicated. Nevertheless, it is important to consider them in these situations. Fortunately, *Gaster* [1962] has considered the problem of the connection between spatial and temporal modes and has developed relations that may be used, in some circumstances, to convert predictions from one into the other. *Dodd and Falqués* [1996] solve the spatial stability problem for realistic longshore current profiles (one on a plane beach and one on a barred beach) and show that the Gaster relations may indeed be used with a high degree of accuracy for shear waves. (The *Bowen and Holman* [1989] solution, however, is singular in the spatial problem, and so the relations are inapplicable here.) Significantly, the barred beach case examined by *Dodd and Falqués* [1996] is that of the first successful experimental study of these motions [see *Reniers et al.*, 1994, 1997].

In Appendix A we give a brief resume of the standard numerical methods used in solving the linear problem. We also outline the main numerical approaches to the fully nonlinear problem, the physical interpretations and implications of which we discuss next.

3. NONLINEAR THEORY AND MIXING BY SHEAR WAVES

Linear theory is necessarily limited by the assumptions underpinning it, namely, that motions are in some sense of small amplitude. However, the e-folding times predicted by linear theory (*Bowen and Holman* [1989] obtain about 300 s for a wave of period 753 s; *Falqués and Iranzo* [1994] obtain a time roughly equal to the wave period) indicate that the assumption of linearity will not remain valid for long. Furthermore, observations of shear waves are surely overwhelmingly of fully developed flows in which finite amplitude effects are of importance.

3.1. Weakly Nonlinear Theories

Some progress has been made by using weakly nonlinear theory, in which the behavior of shear waves close to criticality may be examined. *Dodd and Thornton* [1992] used a weakly nonlinear approach (and a Landau equation [*Drazin and Reid*, 1981]) to describe the early evolution of shear waves. They found that the instability was indeed characterized as being supercritical (i.e., an instability will only develop when dissipation is decreased, or the shear increased, above a critical value). Numerical work [*Falqués et al.*, 1994] confirmed these analytical results. While important, this analytical work is limited by the fact that it only considers the evolution of one wavenumber and its higher harmonics. In reality, we have a continuum of unstable wavenumbers of which k_{FGM} is just the "first among equals" [*Drazin and Reid*, 1981]. This analysis was therefore subsequently extended by *Feddersen* [1998] to Ginzburg-Landau theory, which allows the development of a wave packet, in which there is a single, central mode rather than strictly a single one. Once again, it was shown that the instability is supercritical. Comparisons made by *Feddersen* [1998] of these weakly nonlinear disturbances with similar numerical ones (generated by the model of *Allen et al.* [1996]; see section 3.2) also show quantitative agreement.

A somewhat different approach has been taken by *Shrira et al.* [1997]. Considering the theory of resonant triad interactions, they show that so-called explosive instabilities of the longshore current may occur ("explosive" in the sense that interacting waves grow without bound in a finite time). They analyze the model of *Bowen and Holman* [1989] and identify qualitatively different regions of instability, which they characterize as being (1) linear, (2) nonlinear-S, and (3) nonlinear-U. The linear region is that considered by previous authors, but the nonlinear regimes are new to this field. *Shrira et al.* [1997] state that the role of these nonlinear processes is different: The U-processes, which are present for all sizes of back-shear in the *Bowen and Holman* [1989] model, tend to amplify the growth of already growing perturbations; the S-processes, on the other hand, are expected to be important only for small values of back-shear. Under these latter conditions, when the flow is linearly more stable, these processes are expected to dominate and, in principle, to provide a mechanism by which instabilities may grow even when a flow is linearly stable due to dissipation, provided initial amplitudes are large enough (i.e., a kind of subcritical bifurcation). In illustrating their proposed mechanism, *Shrira et al.* [1997] considered the profile of *Bowen and Holman* [1989], which has no dissipation. Therefore they were able to consider a triad of neutrally stable modes. For realistic longshore current profiles in the presence of dissipative mechanisms, linear studies will only usually permit triads of decaying stable modes, but in this case, too, explosive processes have been shown to occur [*Dodd and Iranzo*, 1999]. Two questions then immediately pose themselves: (1) How big do such finite amplitude perturbations need to be in order for instability to ensue? (2) What natural mechanism could provide that push? Experiments with realistic current profiles and decaying stable triads [*Dodd and Iranzo*, 1999] show that perturbations in the longshore current, which may be

consistent with naturally occurring ones, can lead to subcritical, explosive growth. Other numerical experiments [*Haller et al.*, 1999] show that wave groupiness can induce longshore current perturbations that have a spatial and temporal structure similar to linear shear instabilities of that same longshore current and that, moreover, the forcing scales (ω, k) are similar to those of linear unstable modes. Work in this area continues (see also section 6).

3.2. Fully Nonlinear Studies

Weakly nonlinear analyses can only go so far. In a strongly nonlinear regime a fully nonlinear model must be used. A number of groups have independently advanced these types of analyses to the extent that there is now a much better understanding of these flows.

Falqués et al. [1994] confirmed the theoretical findings of *Dodd and Thornton* [1992]. They examined the case of a plane sloping beach and included the effects of bottom friction and eddy viscosity coefficients (both constant). Using the control parameters developed in the linear part of their study, they showed that instability ensued for the same critical conditions as for the linear case. Although their numerical model was limited to a small number of Fourier modes, and by numerical instabilities, in the extent to which it could simulate strongly nonlinear dynamics, by examining two subharmonics of the wavenumber of the FGM, as well as the corresponding superharmonics, they were able to observe the initial growth of the FGM and thereafter the transfer of energy into other modes, particularly the first subharmonic, and eventually into a steady, modulated oscillation in all modes. Far from criticality they note that the flows are very different from those close to criticality, and in particular that for the highly nonlinear case there is a substantial mean component generated. They also note that the final amplitude of the shear waves in the highly nonlinear case (the simulation was run for 16 hours of real time) is about 20% of the longshore current maximum, V_{max}, consistent with the observations of *Oltman-Shay et al.* [1989] and *Reniers et al.* [1994].

Deigaard et al. [1994] performed a full numerical simulation of the nearshore dynamics on a barred beach [*Putrevu and Svendsen*, 1992], including the wave field and a sediment transport module, with a finite difference model (see section 6 for a description of their sediment transport predictions). In other words, the wave transformation model was run over the solution domain, which generated a radiation stress field, which led to the generation of the longshore current. This kind of numerical study is similar to a wave basin experiment (see section 4.2) so that a uniform longshore current is generated at the upstream boundary, which then becomes unstable within the model domain (see *Damgaard* [1993] for a more detailed description of these experiments). The current exits the domain using a simple extrapolation boundary condition. Deigaard et al. reported numerical boundary effects, which limited the useful length of the model domain. The longshore current grew over about 2000 s of real time, but even before the end of this "ramping-up" period, oscillations very similar to those observed had developed (wavelength 190 m; period 200 s; phase velocity about 55% of V_{max}). A series of experiments was performed, allowing variations in wave conditions, depth over the bar and bottom friction, as well as numerical parameters. The kinematics were a fairly robust feature of each of these experiments. Notably, for a plane beach, which was also examined in their study, no shear waves could be observed. They also examined the effect of alongshore topographical variations on the shear waves (see section 5). Finally, they investigated the effect of shear waves on cross-shore momentum exchange, which they found to be induced by the shear waves at the bar location and offshore of the bar (consistent with the sediment transport predictions); further inshore, momentum transfer was very small. These exchanges, and the overall vorticity field, have been examined in more detail in other nonlinear numerical modeling studies, which we examine next.

Almost from their discovery, shear waves have excited the curiosity of scientists interested in investigating cross-shore momentum exchanges and, generally, the induced mixing of momentum in the nearshore region. This is because in certain areas of modeling, a deficiency has been known for some time. This is most notable in longshore current modeling, in which the cross-shore profile of a longshore current on a plane beach can be accurately modeled using theory stemming back to the theoretical models of *Bowen* [1969], *Thornton* [1970], and *Longuet-Higgins* [1970a, 1970b] and refinements therefrom [see, e.g., *Thornton and Guza*, 1986; *Larson and Krauss*, 1991]. These models have been shown to be accurate in predicting the cross-shore structure of the longshore current on a plane beach with random waves. (The inclusion of dispersive mixing [*Svendsen and Putrevu*, 1994], however, is important on a plane beach subject to monochromatic wave incidence.) However, over a barred beach, models consistently predict two peaks in the profile, due to waves breaking first on the bar and then on the shore face. Observations during the DELILAH field experiment, however, tend to show a single peak, usually somewhere in between those predicted by numerical models. (Observations from SUPERDUCK on October 16 and 18 were an exception to this in that they show a peak on or seaward of the bar [see *Dodd et al.*, 1992].) Lateral diffusion of momentum (diffusive mixing), which is included in some of these models, fails to account for this. In more recent work, *Svendsen and Putrevu* [1994] analyze current dispersion due to the nonuniformity over depth of the wave-generated currents. They note that this gives rise to additional terms in the depth-averaged momentum equations, which alter the longshore current profile (dispersive mixing). Comparison between the laboratory data of *Visser* [1984b] (monochromatic waves on a 1:20 plane beach) and the longshore current as modeled including

the dispersion effects reveals good agreement. However, later work [*Putrevu and Svendsen*, 1997] reveals that mixing is not sufficient to explain the longshore current profile on a barred beach. Therefore this appears only to answer part of the question.

Bowen and Holman [1989] noted the potential for shear waves to provide an efficient mechanism for cross-shore momentum transport. Furthermore, shear waves are thought overwhelmingly to occur on barred beaches. It is straightforward to derive an energy equation describing this mixing process [*Dodd and Thornton*, 1990]. *Putrevu and Svendsen* [1992] went further and estimated the order of magnitude of this mixing term by a scale analysis. *Putrevu et al.* [1998] use a similar approach to examine the effect of eddy viscosity (see section 2.1). They found that within the surf zone it could indeed be large enough, although outside it did not seem to provide enough mixing to explain laboratory observations. *Church et al.* [1992] undertook a linear stability analysis of DELILAH data (see section 4.1) to determine amplitudes of the velocity components due to the shear waves. They did this by calibrating the computed energy density of oscillations (from linear theory) against the observed densities, to compare magnitudes of the cross-shore radiation stress gradients due to the *Thornton and Guza* [1983] model with the analogous terms due to shear waves. They also found that mixing by shear waves can be very large.

Allen et al. [1996] performed a fully nonlinear numerical study with a finite difference model. They adopt an approach similar to *Falqués et al.* [1994] in that they assume the mean momentum balance to be automatically satisfied (and therefore not present in the model equations); that is, the current (potential vorticity) field is decoupled from the wave field. This approach is significantly different from that of *Deigaard et al.* [1994]; their relative merits are discussed in Appendix A. Unlike *Falqués et al.* [1994], they consider a plane beach. They perform a parametric study of the effect of varying dissipation (here bottom friction, parameterized through a term Q) in their model on the flows.

They conduct three sets of experiments, examining progressively larger (alongshore) model domains to see what boundary effects are present. The control parameter Q is then varied, where this variation is expressed as a deviation, $\Delta Q = Q_c - Q$, from critical conditions (where $Q = Q_c$ implies neutral stability, i.e., disturbances neither growing nor decaying), in order to examine different stability regimes in each flow. (The parameter Q also contains the parameterized effects of variations in the (plane) beach slope and, implicitly, of altering the wave conditions (forcing). Thus decreasing Q (destabilizing the flow) is equivalent to decreasing the bottom friction or increasing either the beach slope or the longshore current peak (for constant back-shear).)

They also confirm that at near-critical conditions (small ΔQ), regular disturbances equilibrate with a phase speed of the shear waves close to that predicted by linear theory. This was a generally robust feature of their experiments. For these near-critical experiments the total mean longshore current develops such that the mean profile $V(x)$, which was originally only just unstable (i.e., near-critical), becomes only just stable; that is, the effect of the shear waves is to stabilize the flow, at least in a linear sense, which has also been noted by other authors [*Slinn et al.*, 1998; *Özkan-Haller and Kirby*, 1999]. However, they still find differences due presumably to domain length effects in the longest domain length experiments.

For larger ΔQ the resulting flows are highly dependent on the domain length. The smallest-scale experiments reveal that a sequence of bifurcations on the route to turbulence ($T \rightarrow 2T \rightarrow 4T \rightarrow 6T$, where T represents the initial period of the disturbance), before turbulence, or at least irregular oscillations, are arrived at, which, as *Allen et al.* [1996] point out, is different from the Feigenbaum scenario of period doubling bifurcations. On the other hand, the nature of these experiments (the numerical model domain length set equal to the wavelength λ_{FGM} of the most unstable mode) prevented subharmonic transitions. In fact, the development of large-scale (i.e., with alongshore length scales substantially greater than those predicted by linear theory), finite amplitude disturbances, which also propagate more slowly than linear waves, is a robust feature of the more realistic experiments, particularly those on a barred beach [see *Slinn et al.*, 1998; *Özkan-Haller and Kirby*, 1999]. It would seem that subharmonic transitions are therefore important to these types of flows. As ΔQ is increased further, the flows become more irregular. A number of different disturbances at different length scales coexist, with the smaller-amplitude disturbances propagating faster than the larger ones. In fact, the smaller-amplitude ones are formed in between larger ones and tend to merge with them when they catch up. The overall width of the mean longshore current increases with increasing instability. Spectral analysis of the most realistic model runs appears to indicate that the observations of *Oltman-Shay et al.* [1989] are at least not of weakly nonlinear waves, although it is difficult to be more certain than this, not least because *Allen et al.* [1996] only examine a plane beach.

Slinn et al. [1998] extend the study of *Allen et al.* [1996] to look at a barred beach. Their study reveals qualitative differences between (numerical) finite amplitude shear waves on barred beaches and those on plane beaches. They examine two barred beach profiles based on measured beach profiles from SUPERDUCK. (*Slinn et al.* [1998] actually use an analytical profile that closely resembles those measured during SUPERDUCK and DELILAH.) The resulting longshore current profile without shear waves is a twin-peak profile, with one peak in $V(x)$ over the bar and another at the shore. Their parametric study reveals that in more nonlinear regimes (larger ΔQ) energy is spread to higher wavenumbers and not primarily lower ones, as found by *Allen et al.* [1996]

for a plane beach. (*Slinn et al.* [1998] use a Q identical to that of *Allen et al.* [1996]. In some of their figures reproduced here, however, they give bottom friction in terms of a dimensional coefficient μ (m s^{-1}), which is the same parameter as that present in (13); they do not use an equivalent to c_d. *Özkan-Haller and Kirby* [1999] use an identical dimensional coefficient μ and relate it to c_d (c_f in their paper) by $\mu = (2/\pi)c_d U_0$, where U_0 is the amplitude of the horizontal orbital velocity of the incident waves.) It is not clear what the primary reason is for this qualitative difference, although the presence of the bar, according to *Putrevu and Svendsen* [1992], tends to confine linear disturbances and may favor smaller-scale disturbances. It is notable, however, that their numerical model does not include the effects of eddy viscosity [see *Özkan-Haller and Kirby*, 1999].

Slinn et al. [1998] identify four separate regimes of longshore shear flow: (1) weakly nonlinear; (2) fluctuating vorticity waves, comprising mostly distinct vortices propagating alongshore at nearly constant phase speed, but which occasionally coalesce; (3) shedding of vortex pairs, where vortex pairs of opposite signs break away and propagate offshore; and (4) turbulent shear flow. Spectral analysis also points to a more nonlinear (or at least not weakly nonlinear) regime as being most reminiscent of observations. This change in the flow as it moves into a gradually more unstable regime is illustrated in Plate 1, which shows snapshots of vorticity associated with the disturbances on two different barred beaches, the first, beach 1, chosen so as to be representative of the bathymetry during SUPERDUCK, and the second, beach 2, similarly representing conditions during DELILAH. The corresponding $\omega - k$ plots are given in Figure 9 and Figure 10, respectively. The simulations of *Slinn et al.* [1998] in more stable regimes tend to show two rows of vortices, one positive (nearer the shore) and one negative (on the back-shear of the mean current), but in some circumstances with one row dominating, the other being more of a vortex sheet (compare the simulations in the top and bottom panels of Plate 1). The two rows of vortices appear to be associated with separate potential vorticity extrema, corresponding to shoreward (positive) and seaward (negative) facing shears of the longshore current, about which positive and negative vorticity, respectively, is exchanged. This behavior can also be observed in plane beach simulations [see *Allen et al.*, 1996; *Özkan-Haller and Kirby*, 1999] when the assumed longshore current profile also possesses two such extrema. In a large eddy simulation, *Sinding et al.* [1995] also reported observing two rows of vortices on a barred beach, each with opposite rotations, like those in the simulations shown here. On a plane beach, in contrast, the shear waves are associated with a single row, located offshore of the position of V_{max}. It is not known, however, what kind of current profile their simulations corresponded to.

Slinn et al. [1998] also found that shear waves extensively "fill in" the velocity deficit originally present in the longshore current profile. In other words, they provide a potent source of momentum mixing, as thought by earlier authors. They also note that a subsequent linear stability analysis of mean weakly nonlinear profiles (which implicitly include equilibrated shear waves) reveals that they have been stabilized, as was also found by *Allen et al.* [1996]. A similar linear analysis of mean flows derived from strongly nonlinear flows showed good agreement with propagation velocities and alongshore wavelengths obtained from running a nonlinear instability simulation of the initial (unmixed) profile [see *Dodd et al.*, 1992], implying, again, that the observations made by *Oltman-Shay et al.* [1989] are most likely of fully nonlinear shear waves, although a detailed comparison of observations and numerical simulations was still lacking at this point.

At SUPERDUCK it was observed that the peak in the longshore current profile was mostly situated over the bar, rather than over the trough, as is sometimes observed. This variability in the maximum of $V(x)$ has been noted previously [*Sallenger and Howd*, 1989]. Conducting investigations into the effect of the relative position of the peak is therefore relevant [*Putrevu and Svendsen*, 1992], although, of course, in the presence of shear waves the observed profile will be "mixed" already. *Özkan-Haller and Kirby* [1999] (using a numerical model developed earlier [see *Özkan and Kirby*, 1995; *Özkan-Haller and Kirby*, 1996]) perform a numerical simulation of shear waves including the effects of bottom friction and lateral momentum mixing, like *Falqués and Iranzo* [1994], but also incorporating the dispersive effect studied by *Svendsen and Putrevu* [1994] in a simplified form. They also incorporate the time-dependent movement of the free surface into their simulations. Their approach is similar to that of *Dodd et al.* [1992] in that they examine field measurements directly (measurements from 3 days from SUPERDUCK), so this work directly addresses the aforementioned gap. Instead of varying the dissipation parameters to examine their effect, they calibrate model parameters against observations. To do this, they first fix their mixing coefficient (M) (see *Özkan-Haller and Kirby* [1999] to see how this dimensionless coefficient relates to ν) and vary the bottom friction coefficient (c_d) in order to see which value best reproduces the observed propagation velocities of the shear waves from those days. They find that a value of c_d between 0.002 and 0.0035 gives the best fit. Their generated time series of alongshore and cross-shore velocities, however, are noticeably different from those recorded and show an intermittent character that was not evident from the original time series, and as well are of longer period. The overall behavior for all simulated days was of a type characterized as being turbulent shear flow by *Slinn et al.* [1998].

They then do the same, holding c_d constant and varying M. The effect of increasing M on the time series is to significantly decrease the high-frequency content of the signals, but the propagation speed is not strongly

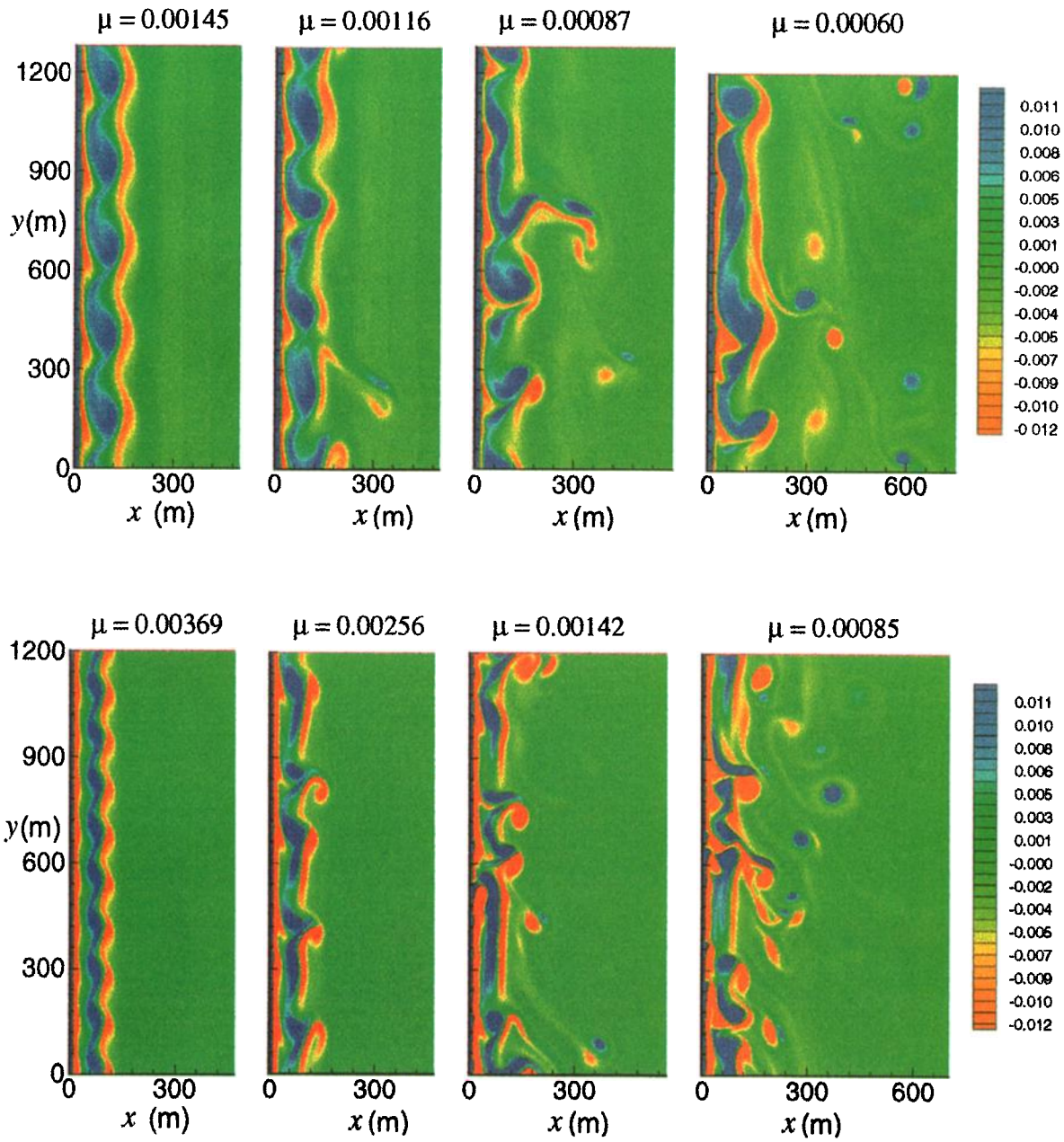

Plate 1. Contour plots of vorticity $\zeta(x, y, t)$ (s^{-1}) fields at (top) t = 15.3 hours for experiments on beach 1 and (bottom) t = 10 hours for experiments on beach 2, with different values of μ ($m\ s^{-1}$). The blue contours indicate positive vorticity (counterclockwise rotation), the yellow and red regions represent negative vorticity, and the green background regions have near-zero vorticity. After *Slinn et al.* [1998].

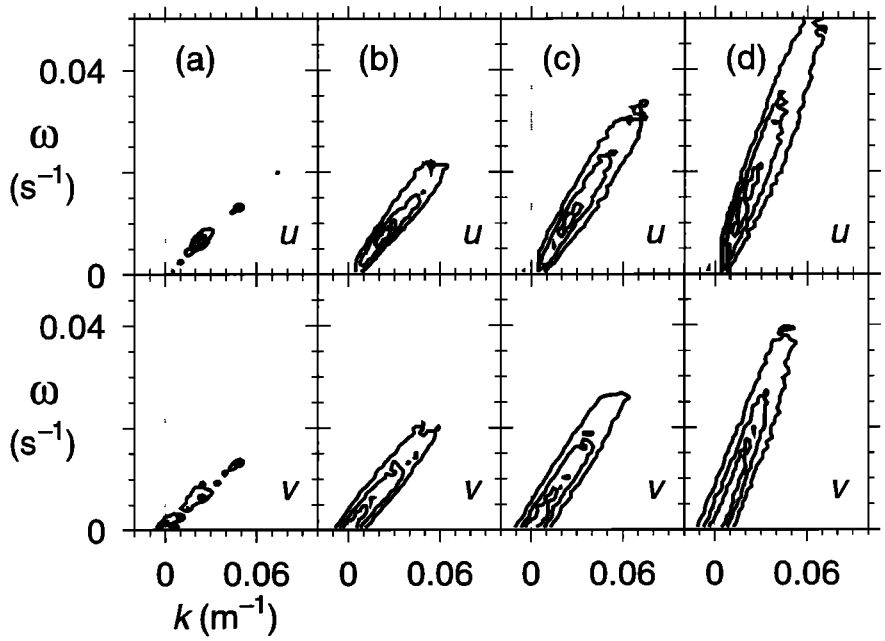

Figure 9. Alongshore frequency-wavenumber ($\omega - k$) spectra for (top) the cross-shore velocity and (bottom) alongshore velocity from experiments on beach 1, for (a) μ = 0.00145, (b) μ = 0.00116, (c) μ = 0.00087, and (d) μ = 0.00060 (m s^{-1}). The spectra are calculated over an 18-hour portion of the experiments (t = 2–20 hours) at locations on the seaward facing side of the bar. Contour levels are 10^{-1}, 10^{0}, and 10^{1} s^{-2}. After *Slinn et al.* [1998].

dependent on eddy viscosity. Increased mixing also strongly affects the tendency of the mean flow to shed vortices, so that as M is increased, the overall length scales of the disturbances increase (i.e., there is a frequency downshift). This favoring of lower frequencies on a barred beach is a robust feature of all these numerical simulations. The effect of varying eddy viscosity is shown very clearly in Plate 2, in which simulations based on 1

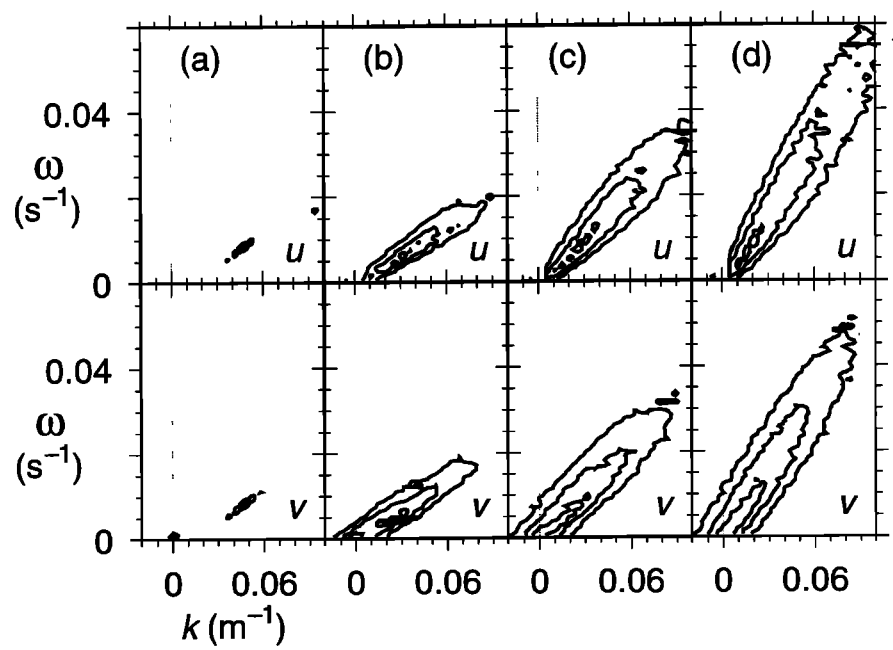

Figure 10. Alongshore frequency-wavenumber ($\omega - k$) spectra for (top) the cross-shore velocity and (bottom) alongshore velocity from experiments on beach 2, for (a) μ = 0.00369, (b) μ = 0.00256, (c) μ = 0.00142, and (d) μ = 0.00085 (m s^{-1}). The spectra are calculated over an 18-hour portion of the experiments (t = 2–20 hours) at a location on the seaward facing side of the bar. Contour levels are 10^{-1}, 10^{0}, and 10^{1} s^{-2}. After *Slinn et al.* [1998].

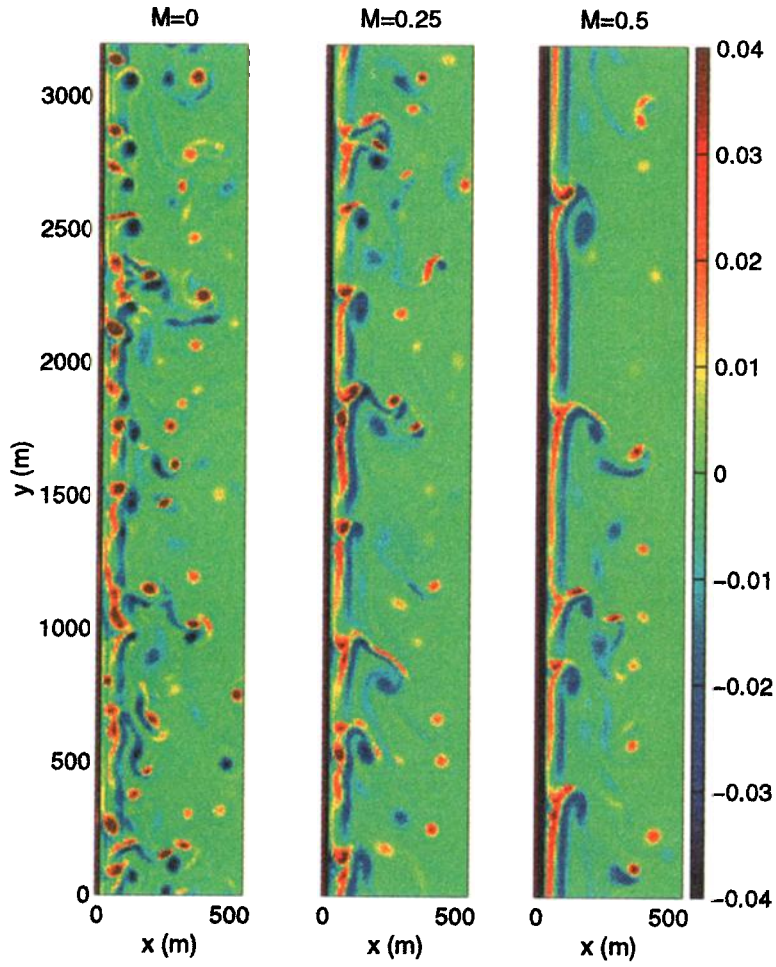

Plate 2. Contour plots of vorticity (1/s) at $t = 5$ hours, for bottom friction coefficient $c_d = 0.003$ and representing conditions on October 18, for different values of eddy viscosity coefficient M. From *Özkan-Haller and Kirby* [1999].

day at SUPERDUCK are shown. Results of simulations for all 3 days of SUPERDUCK examined by *Özkan-Haller and Kirby* [1999] are summarized in Figure 11, in which the simulated and recorded spectra are shown. Here a value of $M = 0.25$ has been used, but it should be noted [*Özkan-Haller and Kirby*, 1999] that this does not represent a "best fit," partly because measurements during SUPERDUCK were primarily from the trough of the barred beach. At that location the effect of varying M on the wavenumber-frequency spectrum was small, thus making it difficult to obtain a best fit.

An important, if slightly disappointing, feature of these studies [see *Slinn et al.*, 1998; *Özkan-Haller and Kirby*, 1999] is that although shear waves are an important source of mixing, they do not appear to provide all the missing mixing. In particular, shear waves do not appear able to explain the shift in the position of V_{max} from the bar to the trough, which is frequently observed. Analysis of results from the laboratory investigation of *Reniers et al.* [1997; see also *Reniers and Battjes*, 1996], although revealing the expected buildup of shear wave intensity in the downstream direction, with the eventual cross-shore momentum flux being something like that predicted by *Church et al.* [1992] (though in this case the contribution in the trough seems to be considerably less), also failed to show significant changes in the mean longshore flow due to shear wave mixing (see section 4 for a description of this experiment). However, two longshore current peaks have been observed during laboratory dye experiments [*Reniers and Battjes*, 1997a], and it appears that such "dual-peak" currents can also be observed in the field when a mean alongshore pressure gradient is absent (A. J. Reniers et al., Effects of alongshore nonuniformities on longshore currents measured in the field, submitted to *Journal of Geophysical Research*, 1999) (see also *Sallenger and Howd* [1989] and section 6).

Özkan-Haller and Kirby [1999] also observe that the final mean longshore current profiles (including instabilities) obtained for three different values of M (including $M = 0$) were very similar, although in the absence of mixing there was a marked increase in the kinetic energy of the perturbations. The effect of the shear waves in this case was strongly to mix the alongshore momentum,

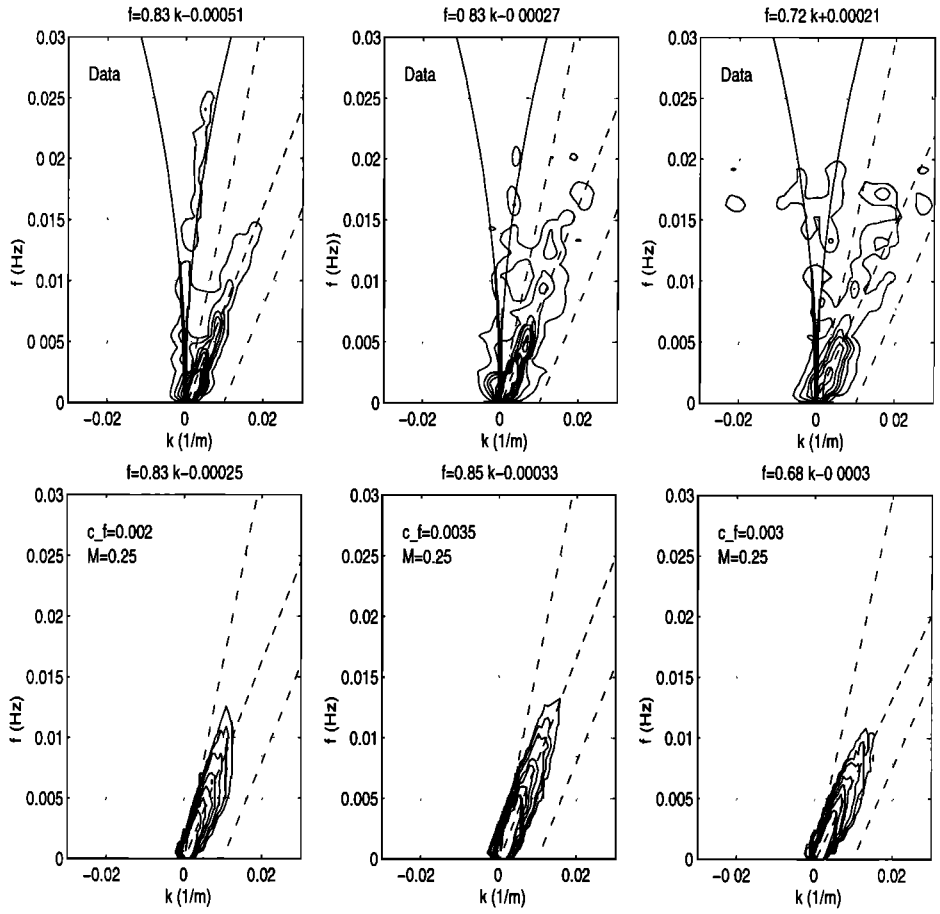

Figure 11. Frequency-cyclic wavenumber spectra $S(f, k)$ ($m^3\ s^{-1}$) for measured and computed longshore velocity at 35 m for (left column) October 15, (middle column) October 16, and (right column) October 18. The estimated shear wave velocity (data, $c_{est} = 0.83$ m s^{-1} for October 15; $c_{est} = 0.83$ m s^{-1} for October 16; $c_{est} = 0.72$ m s^{-1} for October 18; computed, $c_{est} = 0.83$ m s^{-1} for October 15; $c_{est} = 0.85$ m s^{-1} for October 16; $c_{est} = 0.68$ m s^{-1} for October 18) was used to produce the upper and lower cutoff (dash-dotted) lines. The equation for the "best fit" dispersion (dashed lines) line is noted above each plot. Contour levels plotted are 10, 30, 60, 100, 200, 400, and 800. Solid lines are the leaky-trapped boundary. After *Özkan-Haller and Kirby* [1999].

reducing the longshore current peak over the bar and increasing that in the trough.

The complicated vortical structures generated in the simulations of *Slinn et al.* [1998] and *Özkan-Haller and Kirby* [1999] can be seen in Plates 1 and 2. The detailed dynamics of these vortices are illustrated further in Plate 3. Here vorticity is shown as a function of the alongshore coordinate (y) and time at one cross-shore location for about 5 hours of one simulation from October 18 at SUPERDUCK. The vortex interactions are evident and consist primarily of a smaller, faster vortex catching up with a larger, slower one. As the smaller vortex collides with the larger one, it immediately becomes larger and slows down, whereas the initially larger, more coherent structure loses most of its energy and speeds up. The smaller, faster vortices in Plate 3 mostly possess negative vorticity, opposite to the larger structures, although other simulations have similar collisions where both vortices have the same rotation. This process is described in detail by *Özkan-Haller and Kirby* [1999]. To the observer the result is a large coherent vortex, which undergoes a small phase shift (as the collision occurs). In effect, the vortices exchange identities, and when the next small, fast vortex encounters the large one, identities are similarly exchanged. The whole process is reminiscent of a group velocity, with the large, coherent vortical structures mostly propagating at fairly constant velocities but with individual, faster vortices being more intermittent in character. This was also noted by *Allen et al.* [1996], who remarked that in a regime between that of finite amplitude, equilibrated waves (which do not collide) and a more irregular regime like that depicted in Plate 3, wave group-like structures were even more evident.

This group-like structure, in which different vortices can possess different speeds, may seem to contradict the nondispersive character of the observations. However, it is important to note that most of the larger vortices are

stable structures and mostly propagate at the same speed; in contrast, the smaller, faster disturbances are ephemeral (see Plates 3 and 4).

This process provides a mechanism by which the length scale of shear instabilities may increase; vortex interactions produce one large structure, with the smaller vortex either decaying or colliding with another larger structure. The main structure of the resulting flow is provided by the large eddies. The simulations of *Allen et al.* [1996] and *Özkan-Haller and Kirby* [1999] on a plane beach (see Figures 8 and 16 of *Allen et al.* [1996] and Plate 4 of the present paper) seem to agree on the vortex dynamics, although *Özkan-Haller and Kirby* [1999] note that some of the smaller vortices disappear. The simulations of *Özkan-Haller and Kirby* [1999] on a barred beach show a much more complicated picture, depending on the amount of eddy viscosity included (compare Plate 3 with Figure 23 of *Özkan-Haller and Kirby* [1999]). Essentially, though, the interactions are similar.

These complicated vortex dynamics were also the subject of speculation as to the generation of vortical, eddy-type motions in the surf zone by other means [*Peregrine*, 1995, 1998a]. Work in this area is discussed in section 5.

4. FIELD OBSERVATIONS, EXPERIMENTAL INVESTIGATIONS, AND CONDITIONS LEADING TO THE FORMATION OF SHEAR WAVES

4.1. Field Observations

The first clear evidence of the existence of shear waves was given by *Oltman-Shay et al.* [1989] (see Figure 2 and section 1). Further evidence from the same site has subsequently been presented [*Dodd et al.*, 1992]. Subsequent field campaigns from the same location (DELILAH [*Crowson et al.*, 1988]; DUCK'94 [*Birkemeier and Thornton*, 1994]; and Sandy Duck) have also revealed abundant evidence of these motions. However, evidence from other sites worldwide has been less forthcoming. *Dodd et al.* [1992] investigated the possible observation of these motions at Leadbetter Beach, California. They examined motions observed during the Nearshore Sediment Transport Study (NSTS) of 1980, but comparisons of theoretical predictions and observations were less conclusive because the observed motions were less coherent than those seen at Duck. However, this relative lack of coherence is consistent with the smaller current shear observed there. Subsequently, *Oltman-Shay and Howd* [1993] have reanalyzed the data from Leadbetter Beach and have shown convincing evidence of shear waves at this site. They show even clearer evidence of such motions from observations made at the Torry Pines field site (also in California) from the same study. Both beaches are notably different from the one at the Duck site, in that they have steeper offshore profiles and are planar (i.e., they have no surf zone bars). The clearer evidence from the Torry Pines site perhaps reflects the shallower surf zone slope there (relative to Leadbetter Beach), although the implied offshore shear is no greater, because the cross-shore extent of the longshore current is much larger [see *Oltman-Shay and Howd*, 1993, Figure 3].

Other, preliminary evidence from the Trabucador Bar off the Spanish coast near Barcelona perhaps indicates the presence of shear waves there [*Falqués et al.*, 1994], but no more than this. *Falqués et al.* [1994] present a stability diagram based on linear theory including both bottom friction and eddy viscosity. This figure (see Figure 12) indicates the "position" of various field sites and laboratory setups in this regime. Interestingly, the analysis of *Falqués et al.* [1994] predicts instability at both the SUPERDUCK and Trabucador Bar sites but stability at Leadbetter Beach. Observations of rip currents, made at La Jolla, California [*Smith and Largier*, 1995], also indicate the possible occurrence of instabilities at this site.

4.2. Laboratory Experiments

The relevance of shear instabilities to laboratory experiments was assessed by *Putrevu and Svendsen* [1992]. They identified typical length scales of O (8 m) and timescales O (20 s) for shear waves based on the earlier experiment of *Visser* [1984b]. In addition, they estimated the temporal growth rate of the shear instabilities, concluding that in the Visser experiment dissipative effects were dominant and therefore suppressed the occurrence of shear instabilities.

A second assessment was made by *Brøker et al.* [1994], who scaled the numerical results of *Deigaard et al.* [1994] to laboratory conditions. They concluded that the length of the basin should be about 50–100 m, if an rms wave height of 10 cm were considered, before shear instabilities would become apparent.

In the spring of 1994, *Reniers et al.* [1994] performed laboratory experiments in a multidirectional wave basin 40 m long by 25 m wide (see Figure 13) to examine the generation, growth, and equilibrium conditions of shear instabilities under controlled conditions. On the basis of previous investigations the bottom profile was optimized and conditions were selected that were considered most conducive to the generation of shear instabilities.

The experiments were conducted with unidirectional monochromatic and random waves with an incidence angle of 30°. Recirculation of the longshore current was provided for by a pump system in order to develop a realistic uniform base flow with a shear structure similar to that in the field [*Visser*, 1984a]. Different incident wave heights, wave periods, and water levels, as well as a barred and nonbarred concrete profile, were used to assess their effect on the shear instabilities [see *Reniers et al.*, 1997, Table 2]. To look for shear instabilities, spectral analyses in the frequency and frequency-wavenumber domain of the current velocity time series obtained with the current meters in the spatially lagged longshore arrays were performed. An example of an f–k_y spectrum, obtained for a test with random waves, is shown in Figure 14 (note that here $k_y \equiv k$). The area in between the zero-mode edge wave dispersion curves represents

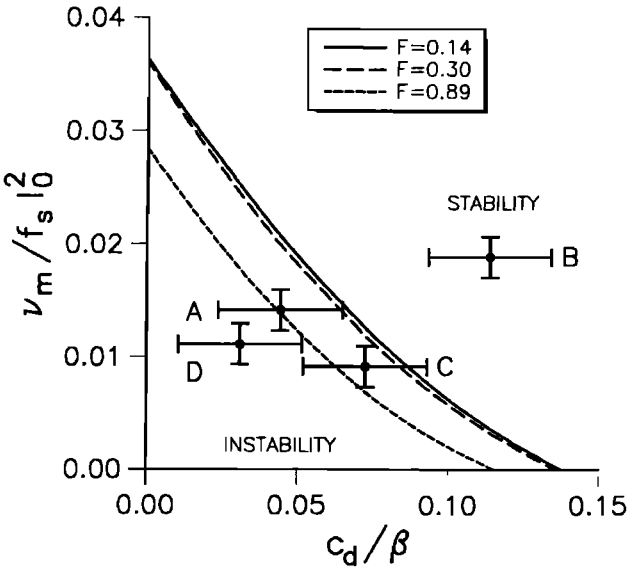

Figure 12. Stability diagram showing boundary between stable and unstable regions as a function of an eddy viscosity (ν_m) parameter (where f_s is the longshore current back-shear and l_0 is the surf zone width) and a bottom friction parameter (where β is the beach slope) for three different Froude numbers. Also indicated are the positions in this space of four separate observational/experimental data sets (with approximate uncertainty estimates): A, Duck (United States); B, Leadbetter (United States); C, wave basin experiment Large Installations Plan (LIP) project M19; and D, Trabucador (Spain). Reprinted from *Falqués et al.* [1994] with permission from the American Society of Civil Engineers.

energy density associated with gravity waves. The observed shear instability energy density is clearly outside this domain. For regular wave conditions the energy density within the gravity wave domain was negligible.

Shear instabilities occurred in all the cases where a barred profile was used. The mixing associated with the presence of shear instabilities is shown in Figure 14, in which the momentum flux $R(x_i)$ at a cross-shore location in a single transect is shown ($R = \rho h(x_i) \langle u(x_i, t), v(x_i, t) \rangle$), where ρ is the water density and angle brackets represent a time average. The buildup downstream is evident. For tests with a plane profile, shear instabilities were not detected.

The occurrence of strong vortical motions is apparent from a sequence of snapshots of the surface elevation (see Plate 5). Starting at the upper left panel, we see that after passing the bar crest, waves stop breaking in the trough and propagate farther toward the shoreline, showing curved wave crests due to bottom refraction. Given the decreasing depth from trough to water line, a convex curvature is expected, which is indeed apparent. A few seconds later a local disturbance is present, showing concave instead of convex wave crests (upper right panel of Plate 5), where current refraction due to the presence of shear instabilities takes precedence over bottom refraction. Further in time this oscillation propagates downstream, thereby increasing in magnitude, displaying an increased interaction with the incident wave crests.

5. OTHER CAUSES AND INTERPRETATIONS OF VERY LOW FREQUENCY SURF ZONE CURRENT FLUCTUATIONS

Prior to the discovery of shear waves, infragravity motions were thought primarily to be a result of wave groupiness [see, e.g., *Mase and Iwagaki*, 1986]. However, once infragravity energy was generated, it could reside in

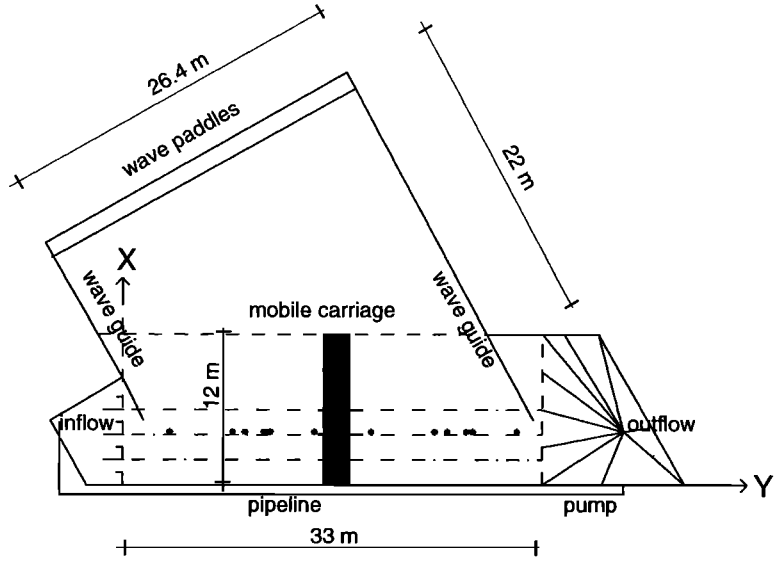

Figure 13. Layout of experiment, including position of current meters in upstream and downstream alongshore arrays, denoted by markers. From *Reniers* [1999].

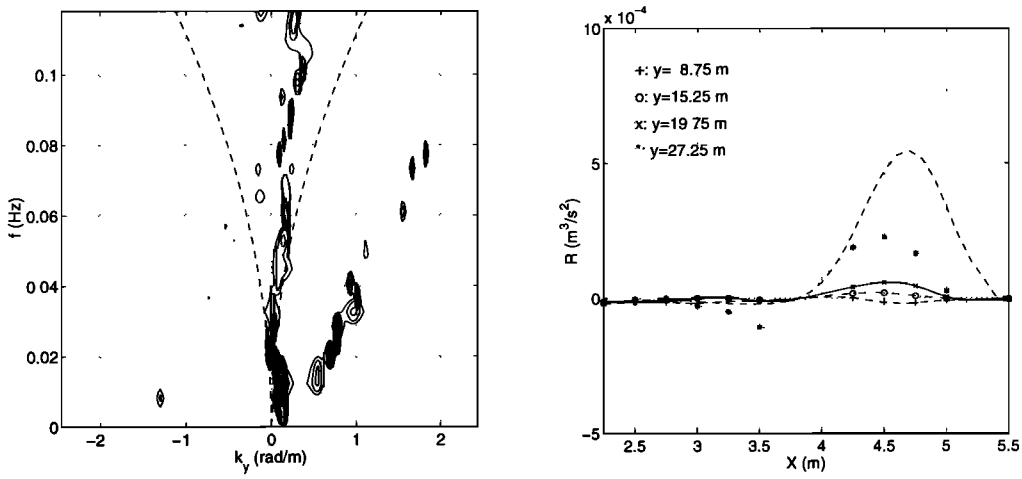

Figure 14. (left) The $f - k_y$ spectrum of alongshore velocity for test SO014 (water depth 55 cm; wave height 8.0 cm; period 1.2 s) obtained from downstream array. Energy density contour lines are at 0.1, 0.2, 0.5, 1, 2, 5, 10, 20, and 50 $(\text{m s}^{-1})^2/(\text{m}^{-1}\ \text{Hz})$. Zero mode dispersion curves obtained for a plain beach (dashed lines) have been added as a reference. (right) Alongshore development of integrated momentum transfer induced by shear instabilities. Distance from inflow is given by y. Measurements (markers) are connected by spline. Estimated wave-breaking induced lateral mixing is given as a reference (dashed line). From *Reniers* [1999].

different types of motions. One of the most investigated has been edge waves [see *Eckart*, 1951; *Huntley and Bowen*, 1973; *Huntley et al.*, 1981; *Oltman-Shay and Guza*, 1987; *Ursell*, 1952], which are trapped gravity modes. In fact, it was the stark difference between the kinematics of shear waves and edge waves that first alerted scientists to this new phenomenon (see section 1). Recently, *Kirby et al.* [1999] have examined the exchange of energy between edge and shear waves. Low-frequency energy can also exist in so-called leaky (non-trapped) modes [see, e.g., *Suhayda*, 1974]. Another possible source of low-frequency energy generation linked to the wave field has been given by *Shemer et al.* [1991], who propose a mechanism stemming from a resonant triad interaction between a wave field and its two most unstable sidebands, which then exhibits a slow-time modulation, and *Tang and Dalrymple* [1989], who examine the effect of intersecting wave trains, which can lead to an alongshore, group-scale modulation of radiation stress field. All these mechanisms rely on the infragravity energy being linked to the wave field, with it being subsequently transferred to the surf zone by some mechanism [see, e.g., *Symonds et al.*, 1982; *Schäffer*, 1993].

An important distinction between these and shear wave motions is that the former are forced phenomena, whereas the latter are free. A discussion of these types of different motions in the context of morphodynamical instabilities is given by N. Dodd et al. (The use of stability methods for understanding the morphodynamical behavior of coastal systems, submitted to *Journal of Coastal Research*, 2000).

More recently, however, the interest in nearshore vortical motions has led to an interest in the direct generation of these motions, particularly by the longshore current shedding eddies. Bed topography is rarely uniform alongshore, except on megatidal beaches, and one result of this is that any significant kink, bump, or hollow can be a source for eddy shedding when a reasonably coherent current passes by; precisely this effect was noted in the numerical model investigation by *Sancho and Svendsen* [1999; see also *Slinn et al.*, 2000].

Deigaard et al. [1994] had earlier investigated imposing alongshore periodic bed perturbations on a shear wave simulation. They discovered that imposing a periodic perturbation on the bar (400 m wavelength) led to the complete suppression of any shear waves when the perturbation amplitude reached 0.4 m (on an unperturbed bar crest depth of 1.5 m). In contrast, *Sancho and Svendsen* [1999] find that a periodic rip channel in a longshore bar acts as a source of destabilization so that shear instabilities are observed sooner, although the average dynamics are unaffected. The rip channels of *Sancho and Svendsen* [1999] are 10% deeper than the unperturbed depth on the bar crest (rip channels of *Deigaard et al.* [1994] have a corresponding depth of 27% of the unperturbed depth). However, it appears that it is the form of the alongshore perturbations that is the cause of the differences, with sinusoidal perturbations of *Deigaard et al.* [1994], in effect, causing the longshore current to become topographically controlled, so no longer prone to instability. In contrast, *Sancho and Svendsen* [1999] use a nonsinusoidal perturbation, in which the rip channels behave much more like isolated channels. In fact, *Sancho and Svendsen* [1999] also investigate nonperiodic disturbances and find little difference between the two. *Slinn et al.* [2000] examine these effects and also conclude that alongshore variability can be an important factor for shear wave dynamics. In a study on the mean longshore current, *Putrevu et al.*

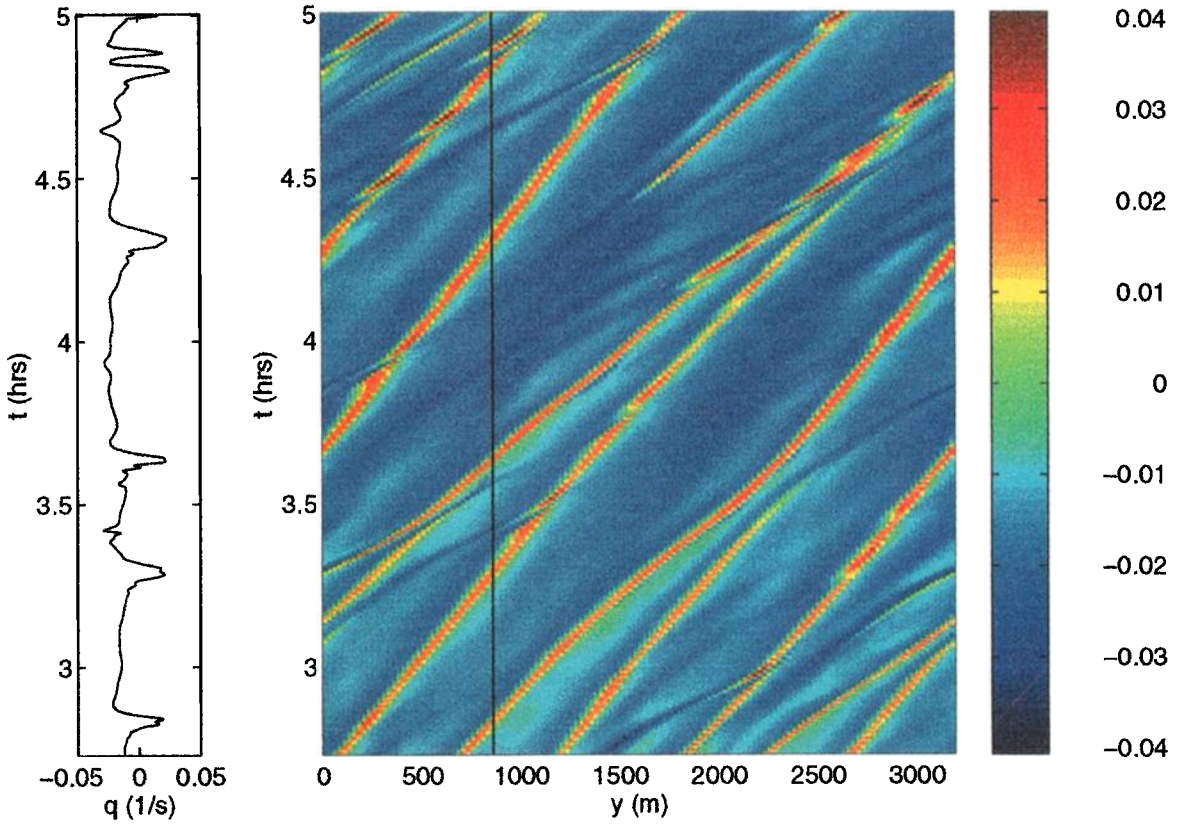

Plate 3. Contour plot of vorticity as a function of the alongshore coordinate y and time t at $x = 100$ m for SUPERDUCK on October 18. Bottom friction coefficient $c_d = 0.003$; eddy viscosity coefficient $M = 0.5$. Left panel shows the time series of vorticity at $y = 900$ m, the location of which is indicated by the solid line in the right panel. From *Özkan-Haller and Kirby* [1999].

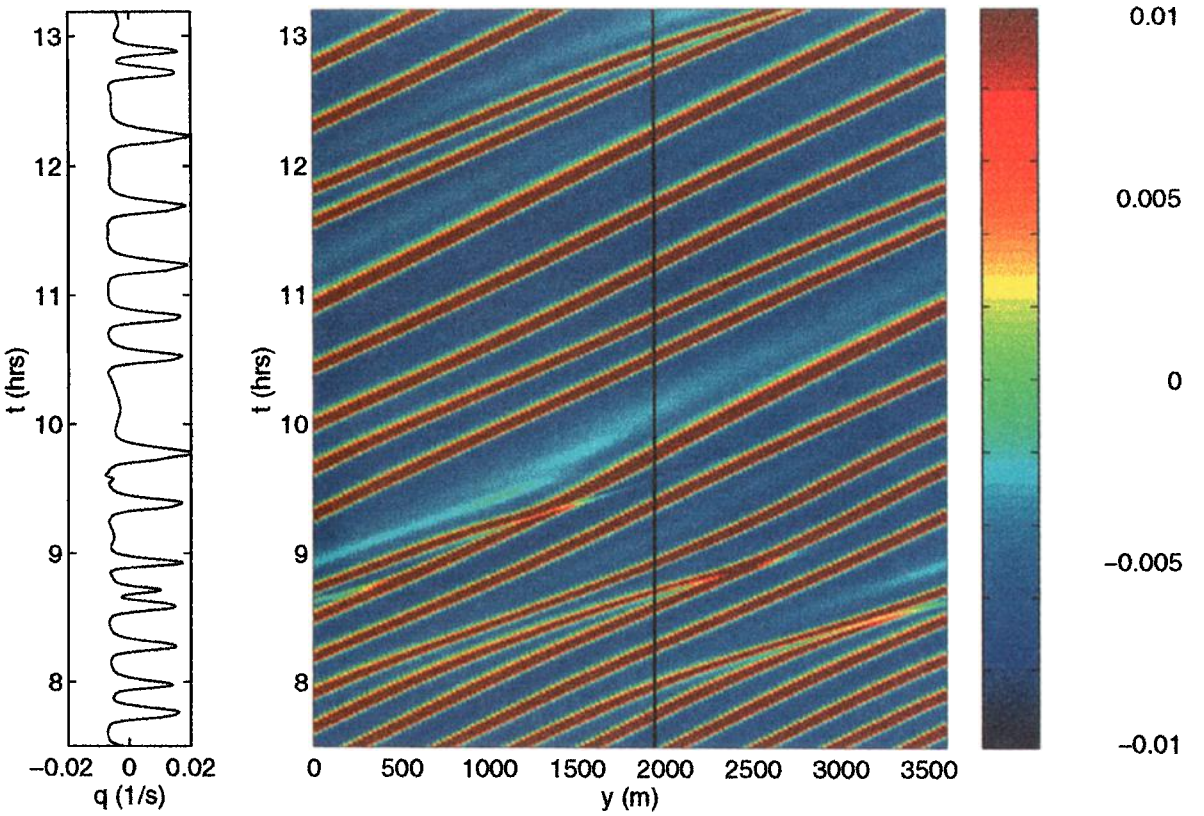

Plate 4. Contour plot of vorticity as a function of the alongshore coordinate y and time t at $x = 90$ m on a plane beach. Left panel shows the time series of vorticity at $y = 1940$ m, the location of which is indicated by the solid line in the right panel. From *Özkan-Haller and Kirby* [1999].

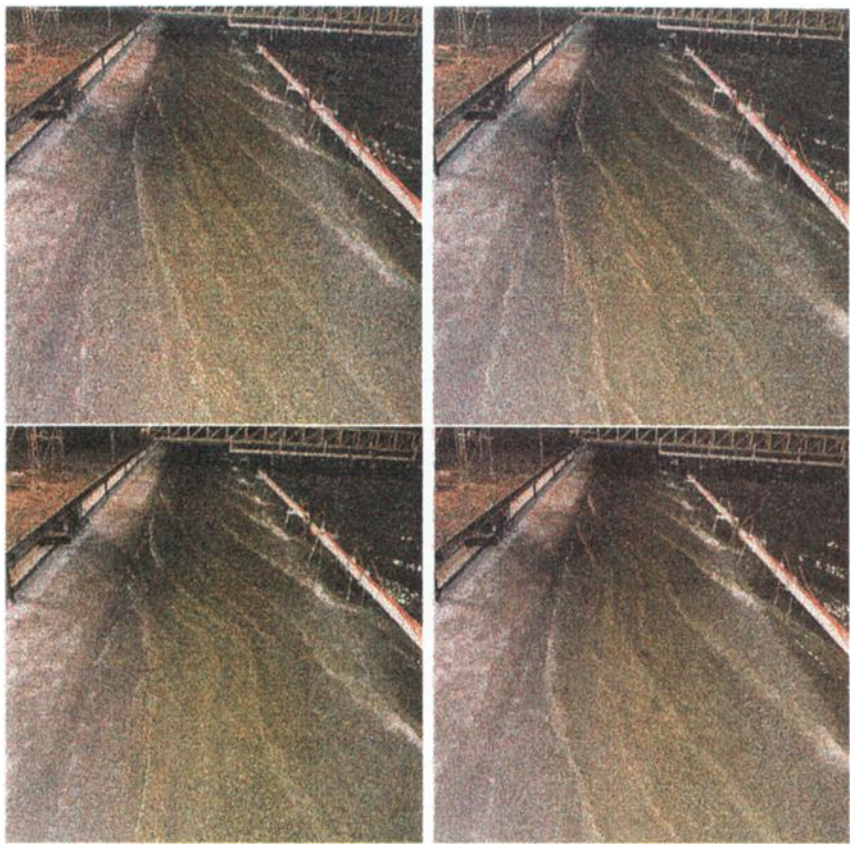

Plate 5. Snapshots with an interval of approximately 4 s (clockwise starting in the upper left panel) of the experimental setup and wave field during test SA243 (regular waves; water depth 55 cm; wave height 8.0 cm; period 1.2 s). From *Reniers* [1999].

[1995] show that deviations of about 10% from alongshore homogeneity can lead to differences of up to 30% in (steady) longshore current predictions. This seems to agree with the findings from the shear wave studies.

Another source of eddies is the edges of breakers [see *Peregrine*, 1998b]. Breakers are, in reality, of finite length, or alternatively they may have gaps within them. There are two reasons for this: (1) The incident waves do not have infinite crests (this cause is rather irregular), and (2) refraction and diffraction can concentrate or diffuse wave energy, leading to enhanced or reduced breaking. This is moderately regular since much refraction and diffraction is due to bottom topography, which changes only slowly (in terms of the usual measurements of currents), if at all. Interestingly, this latter mechanism directly links the wave field to the generation of vorticity in the surf zone.

Finally, flows across the beach due to streams or exits from lagoons can also act as sources of vorticity. These are generally rather obvious but can be expected to be liable to break up into eddies (see the jet flow photographs of *Dracos et al.*, 1992]). *Dodd and Falqués* [1996] also noted this possibility and cited, in particular, coastline interruptions as being possible sources of shear instabilities.

6. FUTURE WORK

So far only *Deigaard et al.* [1994] have examined the capacity for shear waves to transport sediment. They find that instabilities actually reduce longshore transport just shoreward of the bar crest (i.e., at the peak of the longshore transport in the absence of shear waves) by about 17%. The presence of the shear waves also induces a cross-shore sediment transport, the effect of which is primarily to remove material from the shoreward face of the bar, depositing it both farther offshore and on the bar crest. They find a cross-shore sediment transport rate of 1 $m^3\ m^{-1}\ h^{-1}$, which is substantial compared with other contributions. Further work on this aspect and particularly on the capacity of eddies (vortices) to transport suspended sediment or dissolved material would seem important.

On the numerical side, recent computational work by *Allen et al.* [1996], *Slinn et al.* [1998], and *Özkan-Haller and Kirby* [1999] shows frequent development of eddies and interesting behavior of eddies in the nearshore environment. This work should be further developed to gain greater understanding of eddy creation and growth and of the behavior of isolated eddies, pairs of eddies, and collections of eddies in the beach environment.

Once eddies have formed, they move by advection in the current field and by the effect of their "image" in the topography. This latter effect makes eddies tend to follow bed contours. This is not well proven or documented, but for a plane beach there is a family of these eddy-type solutions, of which Hill's spherical vortex [*Lamb*, 1932] is one limit [see *Peregrine*, 1995, 1998a]. This implies that if there is some moderately regular very low frequency fluctuation in a velocity measurement at a point, then one should look "upstream" and along bed contours to see if there is a likely source of eddies. Furthermore, eddies can be expected to have a long life in the surf zone on a gently sloping beach. This nonlinear numerical modeling approach eventually needs to be extended to include feedback onto the wave field.

Work on the effect of alongshore nonuniformity has shown that important dynamics can be missed by assuming alongshore homogeneity [*Sancho and Svendsen*, 1999; *Slinn et al.*, 2000], even though at least to a first approximation the assumption is certainly reasonable. Nevertheless, this area is still relatively unexplored, and it also seems important that mean alongshore gradients (albeit very small ones) should be investigated. Such gradients may indeed account for some "anomalous" mean longshore current profiles (in that the position of $V_{\max}$ may not be where it is expected), and the shear instability climate may be different in such cases, where the profile is not wholly determined by the wave forcing.

On the theoretical side, there would appear to be a number of areas still ripe for exploration, notably further investigation of growth by resonance and subcritical bifurcations [*Shrira et al.*, 1997] and of energy exchanges between shear waves and other forms of nearshore motions (e.g., edge waves) [*Kirby et al.*, 1999].

Perhaps the biggest challenge, however, is to measure velocities over the whole surf zone at once, preferably in such a way that the incident wave motions can be separated out, in other words, to obtain the kind of synoptic view of surf zone currents and structures presently provided by numerical models. The impressive recent work on video imaging [*Holman*, 1993] is, at present, of comparatively little use for giving a picture of the surf zone circulation. Acoustic Doppler techniques can work where there is little air entrainment and perhaps could be tried on the laboratory scale. Overall future developments should lead to more detailed knowledge and a better understanding of the coherent structures of the surf zone.

APPENDIX A: NUMERICAL METHODS

Two different classes of problems are considered here: (1) linear stability analysis and (2) nonlinear temporal evolution.

A1. Linear Problem

The linear stability analysis solves numerically the eigenvalue problem defined by (8) or its various extensions and counterparts. It reduces to determining the eigenvalues and eigenfunctions given a value for k (for the spatial stability problem the roles of ω and k are reversed). If the rigid-lid assumption is applied, only one equation need be solved (an equation like (8) for potential vorticity). Three different techniques have so far been used: a finite difference discretization, a spectral discretization, and a shooting method.

Finite difference schemes and spectral methods consider the discretized eigenvalue problem as a system of algebraic equations $A\tilde{\Psi} = \omega B\tilde{\Psi}$, where the boundary conditions are introduced as a part of the system. Both techniques simultaneously find the $n - n_{bc}$ eigenfunctions and eigenvalues, where n is the number of finite difference nodes (spectral method collocation points) and n_{bc} is the number of boundary conditions. In both methods, therefore, the number of eigenfunctions/values is proportional to the accuracy (as opposed to the order) of the discretization, so it is important to distinguish physical and numerical (or spurious) eigenmodes. Fortunately, this is typically easy to do, not least because the physically important modes are usually those with the largest growth rate, and can be achieved simply by increasing the number of nodes (points) and noting the convergence (or otherwise) of the eigenvalues. The advantage of the spectral method over the finite difference method is the smaller number of points usually needed (compared with finite difference nodes) because they can be tailored to suit the problem in hand [see *Falqués and Iranzo*, 1994; *Özkan-Haller and Kirby*, 1997b]; however, finite difference methods are usually more robust and easier to program. The finite difference discretization is achieved by central differencing; see *Dodd et al.* [1992] (second-order accuracy) and *Putrevu and Svendsen* [1992] (fourth-order) among others.

Spectral schemes for these problems are more diverse [see *Boyd*, 1987; *Canuto et al.*, 1987]. *Falqués and Iranzo* [1994; see also *Iranzo and Falqués*, 1992] use a domain decomposition technique, where the rational Chebyshev collocation scheme [*Boyd*, 1987] and common Chebyshev techniques for finite intervals [*Canuto et al.*, 1987] are combined in order to reach the highest resolution at the peak and at the sea face of the mean velocity profile. The integration domain $[0, \infty)$ is cut into two parts: $[0, L_1)$ and $[L_1, \infty)$. Then Chebyshev collocation is used in the finite part and rational Chebyshev is used in the infinite one. Since a system of second-order ordinary differential equations is considered, the continuity of the solution $\tilde{v}(x)$ and its derivative $d\tilde{v}(x)/dx$ has to be imposed at the matching point $x = L_1$. Both intervals are mapped onto the interval $[-1, 1)$, and the differential equation is discretized at Gauss-Lobatto nodes. A similar approach is taken by *Özkan-Haller and Kirby* [1997a] (although they solve the nonlinear problem; see

below). The Chebyshev collocation calculations can be carried out efficiently using a fast Fourier transform.

Although finite difference or spectral methods are frequently adequate, neither is accurate compared with shooting methods. *Dodd et al.* [1992] used these methods to provide highly accurate estimates for eigenvalues/functions [see also *Falqués and Iranzo*, 1994]. A drawback is that they usually require a good estimate of the eigenvalue before convergence can be achieved. Once an eigenvalue has been identified, however, local Taylor approximations can be used to estimate neighboring values, and highly accurate estimates for dispersion curves are thus produced; spectral/finite difference methods often fail to do either for small values of k or for values of k such that $\omega_i = 0$. Another problem is that they are sensitive to discontinuities in the coefficients of the equations (i.e., in the longshore current or depth profile, or their first- or second-order derivatives) [see *Dodd et al.*, 1992]. Therefore cubic splines or some other method of constructing smooth profiles must be used. These methods require the second-order (or if eddy viscosity is included, fourth-order) ordinary differential equation (ODE) to be rewritten as a system of first order ODEs [see *Press et al.*, 1992]. Note that both spectral and shooting methods have also been used to solve the spatial stability problem [see *Dodd and Falqués*, 1996].

A2. Nonlinear Evolution

Fully nonlinear shear wave models fall under the much wider heading of partial differential equation solvers. Therefore we do not attempt to give this topic any more than a cursory treatment. Because of the complexity and differences of the models and the different problems so far solved, it is impossible to judge one against the other.

Spatial discretization of the momentum and mass conservation equations has been achieved by either finite difference [*Allen et al.*, 1996; *Slinn et al.*, 1998] or spectral methods [*Falqués et al.*, 1994; *Özkan-Haller and Kirby*, 1996, 1999]. However, the full nonlinear problem introduces a decision about how to represent the alongshore dependence, and because of the qualitative difference between alongshore and cross-shore directions, this varies somewhat. *Özkan-Haller and Kirby* [1997a], who describe the details of the approaches used in other studies of theirs, use alongshore Fourier decomposition and cross-shore Chebyshev representation and go further and relax the rigid-lid assumption and allow for a moving shoreline (although in their shear wave computations [*Özkan and Kirby*, 1995; *Özkan-Haller and Kirby*, 1996, 1999] they do not include the moving shoreline). They achieve this by two coordinate transformations: the first from the physical domain with the moving boundary at one edge, to a fixed domain, and the second from a semi-infinite to a finite domain. The sensitivity of the spectral method to boundary conditions [*Canuto et al.*, 1987] is circumvented by use of the characteristic form for the partial differential equations, as is usual in wave and shock modeling codes.

Other models, based on combining existing hydrodynamical software, have also been used successfully [see *Damgaard*, 1993; *Deigaard et al.*, 1994; *Reniers and Battjes*, 1997b], as have large eddy simulation models [*Nadaoka and Yagi*, 1993; *Sinding et al.*, 1995; *Yagi and Nadaoka*, 1997].

The aforementioned two approaches are periodic by implication because of the Fourier decomposition. *Allen et al.* [1996] and *Slinn et al.* [1998] solve the full nonlinear problem with the rigid lid imposed using finite difference methods. They impose periodic boundary conditions and experiment numerically for any domain dependence. They also introduce a biharmonic diffusion term into the momentum equations to damp numerical instabilities. *Özkan-Haller and Kirby* [1997a] deal with numerical instabilities by a high-order filtering technique [see *Shapiro*, 1970].

For the time integration, codes seem predominantly to have made use of predictor approaches (*Allen et al.* [1996] and *Özkan-Haller and Kirby* [1997a] for Adams-Bashforth second and third order, respectively). These approaches have all the advantages (explicit; stable for nonstiff systems (note that no corrector steps are apparently included in these approaches)) and disadvantages (multi-time-level) traditionally associated with these methods [see *Press et al.*, 1992]. *Falqués et al.* [1994] use a semi-implicit Euler scheme, with the nonlinear terms therefore being represented at the old time level. Being semi-implicit it is thought to be highly stable.

A3. Modeling Approaches: Coupling With the Wave Field

In the nonlinear shear wave studies discussed in section 3, there are two different types of approaches, aside from differences in numerical schemes, etc. One is to decouple the potential vorticity field from the wave field that originally generates it. This approach is taken by *Falqués et al.* [1994], *Allen et al.* [1996], *Slinn et al.* [1998], and *Özkan-Haller and Kirby* [1999]. The other approach is to retain the coupling. This approach has so far been fully implemented only by *Deigaard et al.* [1994].

In the first approach the equations being solved numerically are the mean continuity and the two momentum equations, whether or not the rigid-lid assumption is imposed [see *Allen et al.*, 1996; *Slinn et al.*, 1998; *Özkan-Haller and Kirby*, 1999] or the potential vorticity equation alone [see *Falqués et al.*, 1994]. The attraction of this approach is that it allows a more efficient and more transparent investigation than the "black-box" type of approach used by *Deigaard et al.* [1994]. The disadvantage is that even though the wave fields used to generate the alongshore current may be realistic and consistent with observations (both *Slinn et al.* [1998] and *Özkan-Haller and Kirby* [1999] go to great lengths to generate physically realistic $V(x)$ profiles for each bathymetry being examined), there will nevertheless be no feedback

onto the wave field. The effect of this feedback can be seen clearly in Plate 5. These "vorticity" models (which include the large eddy simulations of *Nadaoka and Yagi* [1993], *Yagi and Nadaoka* [1997], and *Sinding et al.* [1995]) can then be "tweaked" to examine the effect of, say, reducing or increasing dissipation while retaining the same longshore current profile. (*Dodd* [1994] examined differences between linear stability predictions from coupled and decoupled models (coupled only via bottom friction).) This ability can be very important, because it can give insight into the effect of bottom friction or eddy viscosity. On the other hand, nonphysical results, or at least results that would not be observed in the field, can sometimes then be generated. For instance, the vorticity models can easily be tuned to generate shear waves on a plane beach, simply by reducing dissipation. The model of *Deigaard et al.* [1994], in contrast, did not show such instabilities on a plane beach. Observations tend to tally with there being reduced shear wave activity on plane beaches, although shear waves have since been observed on plane beaches [*Oltman-Shay and Howd*, 1993]. The black-box or full approach can therefore provide a more complete picture.

ACKNOWLEDGMENTS. This paper is based on work in the SASME project, in the framework of the EU-sponsored Marine Science and Technology Programme (MAST-III), under contract MAS3-CT97-0081. The authors thank Rolf Deigaard (Danish Technical University), Ap van Dongeren (Delft University of Technology), Albert Falqués (Universitat Politécnica de Catalunya), Howell Peregrine (University of Bristol), and other members of the SASME project, who gave valuable feedback and made useful suggestions. The generosity of Tuba Özkan-Haller, of the University of Michigan, Don Slinn, of Florida Atlantic University, Rob Holman, of Oregon State University, and Joan Oltman-Shay, of Northwest Research Associates, in making available numerous figures for this article is also gratefully acknowledged.

Tommy Dickey was the Editor responsible for this paper. He thanks H. Tuba Ozkan-Haller and an anonymous referee for technical reviews and an anonymous referee for the cross-disciplinary review.

REFERENCES

Allen, J. S., P. A. Newberger, and R. A. Holman, Nonlinear shear instabilities of alongshore currents on plane beaches, *J. Fluid Mech., 310*, 181–213, 1996.

Birkemeier, W. A., and E. B. Thornton, The DUCK94 nearshore field experiment, in *Proceedings of Coastal Dynamics '94*, pp. 815–821, Am. Soc. of Civ. Eng., Reston, Va., 1994.

Bowen, A. J., The generation of longshore currents on a plane beach, *J. Mar. Res., 27*, 206–215, 1969.

Bowen, A. J., and R. A. Holman, Shear instabilities of the mean longshore current, 1, Theory, *J. Geophys. Res., 94*, 18,023–18,030, 1989.

Boyd, J. B., Orthogonal rational functions on a semi-infinite interval, *J. Comput. Phys., 70*, 63–88, 1987.

Brøker, I., H. Johnson, E. A. Hansen, A. Skou, P. Justesen, and R. Deigaard, Three-dimensional processes along sandy beaches—Dimensions of a coastal facility, in *Proceedings of Coastal Dynamics '94*, pp. 103–113, Am. Soc. of Civ. Eng., Reston, Va., 1994.

Caballería, M., A. Falqués, and V. Iranzo, Shear instability of the longshore current as a function of incoming wave parameters, in *Proceedings of Coastal Dynamics '97*, pp. 446–455, Am. Soc. of Civ. Eng., Reston, Va., 1997.

Canuto, M. Y., A. Hussaini, and T. A. Quarteroni, *Spectral Methods in Fluid Dynamics*, Springer-Verlag, New York, 1987.

Church, J. C., E. B. Thornton, and J. Oltman-Shay, Mixing by shear instabilities of the longshore current, in *Proceedings of the 23rd International Conference on Coastal Engineering*, pp. 2999–3011, Am. Soc. of Civ. Eng., Reston, Va., 1992.

Crowson, R. A., W. A. Birkemeier, H. M. Klein, and H. C. Miller, SUPERDUCK nearshore processes experiment: Summary of studies, *Tech. Rep. CERC-88-12*, Field Res. Facil., Coastal Eng. Res. Cent., Vicksburg, Miss., 1988.

Damgaard, J. S., Numerical modelling of finite amplitude shear waves, M.S. thesis, Tech. Univ. of Denmark, Lyngby, 1993.

Deguchi, I., T. Sawaragi, and M. Ono, Longshore current and lateral mixing in the surf zone, in *Proceedings of the 23rd International Conference on Coastal Engineering*, pp. 2642–2654, Am. Soc. of Civ. Eng., Reston, Va., 1992.

Deigaard, R., E. D. Christensen, J. S. Damgaard, and J. Fredsøe, Numerical simulation of finite amplitude shear waves and sediment transport, in *Proceedings of the 24th International Conference on Coastal Engineering*, pp. 1919–1933, Am. Soc. of Civ. Eng., Reston, Va., 1994.

Dodd, N., On the destabilization of a longshore current on a plane beach: Bottom shear stress, critical conditions, and onset of instability, *J. Geophys. Res., 99*, 811–824, 1994.

Dodd, N., and A. Falqués, A note on spatial modes in longshore current shear instabilities, *J. Geophys. Res., 101*, 22,715–22,726, 1996.

Dodd, N., and V. Iranzo, Subcritical instability of wave-driven alongshore currents (abstract), *Eos Trans. AGU, 80*(46), Fall Meet. Suppl., F513, 1999.

Dodd, N., and E. B. Thornton, Growth and energetics of shear waves in the nearshore, *J. Geophys. Res., 95*, 16,075–16,083, 1990.

Dodd, N., and E. B. Thornton, Longshore current instabilities: Growth to finite amplitude, in *Proceedings of the 23rd International Conference on Coastal Engineering*, pp. 2655–2668, Am. Soc. of Civ. Eng., Reston, Va., 1992.

Dodd, N., J. Oltman-Shay, and E. B. Thornton, Instabilities in the longshore current, in *Proceedings of the 22nd International Conference on Coastal Engineering*, pp. 584–596, Am. Soc. of Civ. Eng., Reston, Va., 1990.

Dodd, N., J. Oltman-Shay, and E. B. Thornton, Shear instabilities in the longshore current: A comparison of observations and theory, *J. Phys. Oceanogr., 22*, 62–82, 1992.

Dracos, T., M. Giger, and G. H. Jirka, Plane turbulent jets in a bounded fluid layer, *J. Fluid Mech., 241*, 587–614, 1992.

Drazin, P. G., and W. H. Reid, *Hydrodynamic Stability*, Cambridge Univ. Press, New York, 1981.

Eckart, C., Surface waves in water of variable depth, *Tech. Rep. Wave Rep. 100, Ref. 51-12*, 99 pp., Scripps Inst. of Oceanogr., La Jolla, Calif., 1951.

Falqués, A., and V. Iranzo, Numerical simulation of vorticity waves in the nearshore, *J. Geophys. Res., 99*, 825–841, 1994.

Falqués, A., V. Iranzo, and M. Caballería, Shear instability of longshore currents: Effects of dissipation and non-linearity, in *Proceedings of the 24th International Conference on Coastal Engineering*, pp. 1983–1997, Am. Soc. of Civ. Eng., Reston, Va., 1994.

Feddersen, F., Weakly nonlinear shear waves, *J. Fluid Mech., 372*, 71–92, 1998.

Gaster, M., A note on the relation between temporally increasing and spatially increasing disturbances in hydrodynamic stability, *J. Fluid Mech.*, *14*, 222–224, 1962.

Haller, M. C., U. Putrevu, J. Oltman-Shay, and R. A. Dalrymple, Wave group forcing of low frequency surf zone motion, *Coastal Eng. J.*, *41*(2), 121–136, 1999.

Holman, R. A., The application of video image processing to the study of nearshore processes, *Oceanography*, *6*, 78–85, 1993.

Holman, R. A., and A. J. Bowen, Beyond infragravity, II, Gee no g (abstract), *Eos Trans. AGU*, *69*(44), 1251, 1988.

Howard, L., Note on a paper of John W. Miles, *J. Fluid Mech.*, *10*, 509–512, 1961.

Howd, P. A., and J. M. Oltman-Shay, Beyond infragravity, III, How big is a FIG? (abstract), *Eos Trans. AGU*, *69*(44), 1251, 1988.

Huntley, D. A., and A. J. Bowen, Field observations of edge waves, *Nature*, *243*, 160–162, 1973.

Huntley, D. A., R. T. Guza, and E. B. Thornton, Field observations of surf beat, 1, Progressive edge waves, *J. Geophys. Res.*, *86*, 6451–6466, 1981.

Iranzo, V., and A. Falqués, Some spectral approximations for differential equations in unbounded domains, *Comput. Methods Appl. Mech. Eng.*, *98*, 105–126, 1992.

Kirby, J. T., U. Putrevu, and H. T. Özkan-Haller, Evolution equations for edge waves and shear waves on longshore uniform beaches, in *Proceedings of the 26th International Conference on Coastal Engineering*, vol. 1, pp. 203–216, Am. Soc. of Civ. Eng., Reston, Va., 1999.

Lamb, H., *Hydrodynamics*, 2nd ed., Cambridge Univ. Press, New York, 1932.

Larson, M., and N. C. Krauss, Numerical model of longshore current for bar and trough beaches, *J. Waterw. Port Coastal Ocean Eng.*, *117*, 18,031–18,042, 1991.

Lin, C., *The Theory of Hydrodynamic Stability*, Cambridge Univ. Press, New York, 1967.

Liu, P. L.-F., and R. A. Dalrymple, Bottom frictional stress and longshore currents due to waves with large angles of incidence, *J. Mar. Res.*, *36*, 357–375, 1978.

Longuet-Higgins, M. S., Longshore currents generated by obliquely incident sea waves, 1, *J. Geophys. Res.*, *75*, 6778–6789, 1970a.

Longuet-Higgins, M. S., Longshore currents generated by obliquely incident sea waves, 2, *J. Geophys. Res.*, *75*, 6790–6801, 1970b.

Mase, H., and M. Iwagaki, Wave group analysis of natural wind waves based on modulational instability theory, *Coastal Eng.*, *10*, 341–354, 1986.

Nadaoka, K., and H. Yagi, A turbulent flow modelling to simulate horizontal large eddies in shallow water, *Adv. Hydrosci. Eng.*, *1B*, 356–365, 1993.

Oltman-Shay, J., and R. T. Guza, Infragravity edge wave observations on two California beaches, *J. Phys. Oceanogr.*, *17*, 644–663, 1987.

Oltman-Shay, J. M., and P. A. Howd, Beyond infragravity, I, "New wave" observations (abstract), *Eos Trans. AGU*, *69*(44), 1250, 1988.

Oltman-Shay, J., and P. A. Howd, Edge waves on nonplanar bathymetry and alongshore currents: A model and data comparison, *J. Geophys. Res.*, *98*, 2495–2507, 1993.

Oltman-Shay, J., P. A. Howd, and W. A. Birkemeier, Shear instabilities of the mean longshore current, 2, Field observations, *J. Geophys. Res.*, *94*, 18,031–18,042, 1989.

Özkan, H. T., and J. T. Kirby, Finite amplitude shear wave instabilities, in *Proceedings of Coastal Dynamics '95*, pp. 465–476, Am. Soc. of Civ. Eng., Reston, Va., 1995.

Özkan-Haller, H. T., and J. T. Kirby, Numerical study of low-frequency surf zone motions, in *Proceedings of the 25th International Conference on Coastal Engineering*, pp. 1361–1374, Am. Soc. of Civ. Eng., Reston, Va., 1996.

Özkan-Haller, H. T., and J. T. Kirby, Shear instabilities of longshore currents: Flow characteristics and momentum mixing during SUPERDUCK, in *Proceedings of Coastal Dynamics '97*, pp. 466–475, Am. Soc. of Civ. Eng., Reston, Va., 1997a.

Özkan-Haller, H. T., and J. T. Kirby, A Fourier-Chebyshev collocation method for the shallow water equations including shoreline runup, *Appl. Ocean Res.*, *19*, 21–34, 1997b.

Özkan-Haller, H. T., and J. T. Kirby, Nonlinear evolution of shear instabilities of the longshore current: A comparison of observations and computations, *J. Geophys. Res.*, *104*, 25,953–25,984, 1999.

Peregrine, D. H., Vorticity and eddies in the surf zone, in *Proceedings of Coastal Dynamics '95*, pp. 460–464, Am. Soc. of Civ. Eng., Reston, Va., 1995.

Peregrine, D. H., Surf zone currents, *Theor. Comput. Fluid Dyn.*, *10*, 295–309, 1998a.

Peregrine, D. H., Large-scale vorticity generation by breakers in shallow and deep water, *Eur. J. Mech. B, Fluids*, *18*, 403–408, 1998b.

Press, W. H., S. A. Teulowsky, W. T. Vetterling, and B. P. Flannery, *Numerical Recipes in FORTRAN: The Art of Scientific Computing*, Cambridge Univ. Press, New York, 1992.

Putrevu, U., and I. A. Svendsen, Shear instability of longshore currents: A numerical study, *J. Geophys. Res.*, *97*, 7283–7303, 1992.

Putrevu, U., and I. A. Svendsen, Dispersive mixing in the nearshore, in *Proceedings of Coastal Dynamics '97*, pp. 207–216, Am. Soc. of Civ. Eng., Reston, Va., 1997.

Putrevu, U., J. Oltman-Shay, and I. A. Svendsen, Effect of alongshore nonuniformities on longshore current predictions, *J. Geophys. Res.*, *100*, 16,119–16,130, 1995.

Putrevu, U., J. T. Kirby, J. Oltman-Shay, and H. T. Özkan-Haller, On the viscous destabilization of longshore longshore currents, in *Proceedings of the 26th International Conference on Coastal Engineering*, vol. 1, pp. 217–229, Am. Soc. of Civ. Eng., Reston, Va., 1998.

Reniers, A. J. H. M., Longshore current dynamics, Ph.D. thesis, Delft Univ. of Technol., Delft, Netherlands, 1999.

Reniers, A. J. H. M., and J. A. Battjes, Cross-shore momentum flux due to shear instabilities, in *Proceedings of the 25th International Conference on Coastal Engineering*, pp. 175–185, Am. Soc. of Civ. Eng., Reston, Va., 1996.

Reniers, A. J. H. M., and J. A. Battjes, A laboratory study of longshore currents over barred and non-barred beaches, *Coastal Eng.*, *30*, 1–22, 1997a.

Reniers, A. J. H. M., and J. A. Battjes, Nonlinear modeling of shear instabilities, in *Proceedings of Coastal Dynamics '97*, pp. 436–445, Am. Soc. of Civ. Eng., Reston, Va., 1997b.

Reniers, A. J. H. M., J. A. Battjes, A. Falqués, and D. A. Huntley, Shear wave laboratory experiments, in *Proceedings of International Symposium: Waves, Physical and Numerical Modelling*, vol. 1, pp. 356–365, Int. Assoc. of Hydraul. Res., Delft, Netherlands, 1994.

Reniers, A. J. H. M., J. A. Battjes, A. Falqués, and D. A. Huntley, A laboratory study on the shear instability of longshore currents, *J. Geophys. Res.*, *102*, 8597–8609, 1997.

Sallenger, A. H., and P. A. Howd, Nearshore bars and the breakpoint hypothesis, *Coastal Eng.*, *12*, 301–313, 1989.

Sancho, F. E., and I. A. Svendsen, Shear waves over longshore nonuniform barred beaches, in *Proceedings of the 26th International Conference on Coastal Engineering*, vol. 1, pp. 230–243, Am. Soc. of Civ. Eng., Reston, Va., 1999.

Schäffer, H. A., Infragravity waves induced by short-wave groups, *J. Fluid Mech.*, *247*, 551–588, 1993.

Shapiro, R., Smoothing, filtering, and boundary effects, *Rev. Geophys.*, *8*, 359–387, 1970.

Shemer, L., N. Dodd, and E. B. Thornton, Slow-time modulation of finite-depth nonlinear water waves: Relation to longshore current oscillations, *J. Geophys. Res.*, *96*, 7105–7113, 1991.

Shrira, V. I., V. V. Voronovich, and N. G. Kozhelupova, On the explosive instability of vorticity waves, *J. Phys. Oceanogr.*, *27*, 542–554, 1997.

Sinding, P., E. D. Christensen, R. Deigaard, J. Fredsøe, E. A. Hansen, and L. Arneborg, Investigation of fully developed unstable longshore current, paper presented at the Copenhagen Conference on Complex Dynamics in a Spatially Extended System, Cent. of Chaos and Turbul. Stud., Univ. of Copenhagen, Copenhagen, Sept. 27–30, 1995.

Slinn, D. N., J. S. Allen, P. A. Newberger, and R. A. Holman, Nonlinear shear instabilities of alongshore currents over barred beaches, *J. Geophys. Res.*, *103*, 18,357–18,379, 1998.

Slinn, D. N., J. S. Allen, and R. A. Holman, Alongshore currents over variable beach topography, *J. Geophys. Res.*, *105*, 16,971–16,998, 2000.

Smith, J. A., and J. L. Largier, Observations of nearshore circulation: Rip currents, *J. Geophys. Res.*, *100*, 10,967–10,975, 1995.

Suhayda, J., Standing waves on a beach, *J. Geophys. Res.*, *79*, 3065–3071, 1974.

Svendsen, I. B., and U. Putrevu, Nearshore mixing and dispersion, *Proc. R. Soc. London, Ser. A*, *445*, 561–576, 1994.

Symonds, G. S., D. A. Huntley, and A. J. Bowen, Two-dimensional surf beat: Longwave generation by a time-varying break point, *J. Geophys. Res.*, *87*, 492–498, 1982.

Tang, E. C. S., and R. A. Dalrymple, Rip currents and wave groups, in *Nearshore Sediment Transport*, edited by R. J. Seymour, pp. 205–230, Plenum, New York, 1989.

Thornton, E. B., Variation of longshore current across the surf zone, in *Proceedings of the 12th International Conference on Coastal Engineering*, pp. 291–308, Am. Soc. of Civ. Eng., Reston, Va., 1970.

Thornton, E. B., and R. T. Guza, Transformation of wave height distribution, *J. Geophys. Res.*, *88*, 5925–5938, 1983.

Thornton, E. B., and R. T. Guza, Surf zone longshore currents and random waves: Field data and models, *J. Phys. Oceanogr.*, *16*, 1165–1178, 1986.

Ursell, F., Edge waves on a sloping beach, *Proc. R. Soc. London, Ser. A*, *214*, 79–97, 1952.

Visser, P. J., Uniform longshore current measurements and calculations, in *Proceedings of the 19th International Conference on Coastal Engineering*, pp. 2192–2207, Am. Soc. of Civ. Eng., Reston, Va., 1984a.

Visser, P. J., A mathematical model of uniform longshore currents and the comparison with laboratory data, *Comm. Hydraul. 84-2*, Dep. of Civil Eng., Delft Univ. of Technol., Delft, Netherlands, 1984b.

Whitford, D. J., and E. B. Thornton, Bed shear stress coefficients for longshore currents over a barred profile, *Coastal Eng.*, *27*, 243–262, 1996.

Yagi, H., and K. Nadaoka, Horizontal large eddy computation of longshore current, in *Proceedings of Coastal Dynamics '97*, pp. 456–465, Am. Soc. of Civ. Eng., Reston, Va., 1997.

N. Dodd, Department of Ocean and Resources Engineering, University of Hawaii at Manoa, Holmes Hall 407B, 2540 Dole Street, Honolulu, HI 96822. (dodd@kona.soest.hawaii.edu)

V. Iranzo, Departament de Física Aplicada, Modul B5, Campus Nord, Universitat Politécnica de Catalunya, Barcelona 08034, Spain.

A. Reniers, Department of Oceanography, Naval Postgraduate School, Monterey, CA 93943.